

Principles for tuning heat zone controllers in a belt furnace through modeling and simulation

Henrik Fryklund



LUND
UNIVERSITY

Department of Automatic Control

MSc Thesis
TFRT-6068
ISSN 0280-5316

Department of Automatic Control
Lund University
Box 118
SE-221 00 LUND
Sweden

© 2018 by Henrik Fryklund. All rights reserved.
Printed in Sweden by Tryckeriet i E-huset
Lund 2018

Abstract

In this thesis the heating area of a belt furnace for annealing metal powder has been modeled. The model was extended with PI-controllers for controlling the energy added to the model. It was simulated with differently tuned controllers to test tuning principles for finding suitable control parameters for the process. The most promising tuning principles was then written as a manual with the aim for process engineers at Höganäs AB.

The process is running on a daily basis with control parameters that causes unnecessary overshoots and oscillations in the system. With updated and more suitable control parameters, the furnace is believed to be more efficient. Höganäs has several processes of the same type which the manual could be applied to.

The process consists of non-linear thermal radiation, conduction and convection. It is very slow and has approximately no dead time, thus excluding many tuning principles that rely on the dead time. The most promising tuning principle to apply is the lambda-tuning principle which is often used in the process industry [Åström and Hägglund, 2006]. Due to the accuracy of the model, the design parameter was chosen to ensure stability and monotonic setpoint changes. The manual can be found in Appendix D.

Acknowledgements

I would like to thank my supervisors Tore Hägglund, Ola Löfgren and Magnus Petterson for all of their guidance and help. If not for their help, this would not have been possible. Further I would like to thank Richard Håkansson at Höganäs for helping me with the tests on the furnace, Martin Andersson at the Division of Heat Transfer for the discussions of the numerical implementation of heat transfer, Mattias Fält at the Division of Automatic Control for helping and teaching me how to optimize Julia code and my brother Fredrik Fryklund for helping and answering my questions regarding FEM. Lastly I would like to thank everyone at Höganäs that I have met for all of their help and the Automatic Control department for their hospitality and exchange of ideas.

Contents

1. Introduction	9
1.1 Background	9
1.2 Höganäs	9
1.3 Purpose	10
1.4 Delimitations	11
1.5 Methodology	11
1.6 Outline	11
2. Automatic Control Theory	12
2.1 Intro	12
2.2 PID-controller	13
2.3 Process characteristics	13
2.4 Approximate M-constrained Integral Gain Optimization (AMIGO)	16
2.5 Lambda Tuning	17
2.6 Skogestad's Internal Model controller (SIMC)	19
3. Thermodynamics	20
3.1 Heat transfer	20
3.2 View factor	22
3.3 Combustion	23
3.4 Stepping through time	23
3.5 Exponential smoothing	25
4. The Process	26
4.1 The Heating	26
4.2 The Cooling	28
4.3 Control	28
5. Modeling	29
5.1 Intro	29
5.2 Simplifications	29
5.3 Disturbances	32
5.4 Modeling process	32
5.5 Validation	37

6. Result	42
6.1 Simulations	42
7. Discussion and Conclusion	49
7.1 Comparison	49
7.2 Most promising tuning principle	50
7.3 Accuracy of model	50
7.4 Future work	50
A. View factor	52
B. Gas composition	55
C. Isolation materials	57
D. Manual for tuning the PID controllers (ENG & SWE)	59
Bibliography	65

1

Introduction

1.1 Background

A belt furnace is a process used for rapid thermal processing through a primary heating chamber. It often uses a conveyor belt to transport material through the furnace. The heat applied is controlled in several zones with different purposes such as pre-heating, heating and cooling. Since the process is often very slow and expensive to perform tests on, it is desirable to create a model of the process and simulate. Thus it might be possible to make the simulations faster than the process and perform tests which otherwise could be expensive or dangerous [Conveyor belt furnace, 2018].

1.2 Höganäs

Höganäs AB is the world leader in the development and manufacturing of metal powders [Höganäs - About Us 2018]. Höganäs AB is an international company with its headquarter in Höganäs in north western Skåne in Sweden. The company was first established in 1797 as a coal mining company and has over the years evolved its production from producing bricks and glazed ceramics to their current business, powder metallurgy. The company has over 1800 employees and production all around the world [Höganäs - About Us 2018].

The metal powder that is produced can be condensed into a single solid mass through a process called *sintering*, which is to put pressure on the powder in a shape to achieve a sought for geometrical form, e.g. gears. The strength of sintered components, even with extremely pure iron powder, is not as strong as milled components. A comparison between milled and sintered gears is that there can be close to zero waste of material with sintering. When milling, larger amounts of metal has to be removed from the initial form and the leftover scraps must then be melted for reuse.

The production line

For the factory in Höganäs, the raw material magnetite is mainly shipped from northern Sweden. The magnetite is stored at the factory before it is purified in tall

rods with coke, derived from destructive distillation of coal [Coke (fuel), 2018], thus creating sponge-like rods. The rods are then cracked into powder. The powder needs to be further purified from contaminants in order for the sintering process to produce yielding results. Through an *annealing* process, the powder is purified from approximately 98 % to 99.9 % [Håkansson and Andersson, 2007]. The process is carried out in a belt furnace that mainly consists of two parts, heating and cooling, see Fig. 4.2. The powder is heated on a conveyor belt in a muffle passing through the furnace. The heating area is divided into zones in which there are burners heating the muffle. Each zone has a top and bottom part with several burners in each, controlled by their own PID-controller with their own set point. The burners are fueled by natural gas, which after combustion creates fumes. There are no physical barriers between the zones, thus heat is able to travel with the fumes along the furnace. This leads to that the zones are coupled with each other. After the heating, the powder is cooled and once the powder has been cooled to a satisfying temperature, it is crushed into powder once again due to some sintering in the heating zones. The powder is then packaged and sold directly to customers or used for pre-mixing with other alloys.

Temperature Control

The importance of keeping the correct temperature in the powder is essential for the annealing process to be successful and efficient, thus saving time and energy. If the conveyor belt were to suddenly stop (belt stop), the system needs to counteract the disturbance immediately and efficiently. The temperature set point for the PID-controllers differ between the heating zones, thus creating a *temperature profile* for the furnace. The temperature profile differ between products, this is due to the physical properties of the material.

1.3 Purpose

To ensure that the system is efficient and that the correct temperature is kept within each zone, the control parameters must be set accordingly. At Höganäs, they use a standard set of control parameters that are almost the same for each controller in the belt furnace, as well in other belt furnaces, with slight modifications. The purpose of this master thesis is to derive a manual to be used by the process engineers at Höganäs AB for tuning the PID-controller parameters for the heating zones in the belt furnace. This is to be done by modeling and simulating the process and evaluating different control tuning principles suitable for PID-controllers and the process dynamics.

The result could make the furnaces more efficient in energy usage, thus reducing the amount of natural gas used which will lower emission of carbon dioxide from the combustion and also the run-time cost.

1.4 Delimitations

The modeling and simulation will be done specifically for belt furnace number 28 (BU28) at Höganäs, as the experiments and evaluation will be conducted on it. The manual for tuning the controllers will though be applicable on other furnaces of the same type at Höganäs. Simplifications of the process will be done regarding the geometry and energy balances in the furnace, thus focusing only on the major dynamics, see Sec 5.2 for details.

1.5 Methodology

The first step was the first literature study conducted on heat transfer theory, finite element methods, radiation heat transfer and earlier thesis of the steady state modeling of the furnace and powder. It was followed by simplification of the model in dialogue with Höganäs. The modeling of the furnace was done part wise and in modules. Tests were conducted on the BU28 for validation data to ensure that the major dynamics were captured by the model. The second literature study took place with focus on different tuning principles applicable on the process. A manual applying the tuning principle was written in English and Swedish with the aim of a process engineer as reader.

1.6 Outline

The thesis first covers some basic control theory and the tuning principles that were applied in Chapter 2. Afterward, Chapter 3 goes through the thermodynamic theory for the heat transfer that takes place in the furnace and the implementation of it with the finite element method. Chapter 4 covers how the process works at the level that is needed for the modeling. Chapter 5 goes through the simplifications that were made to the process for the modeling and the energy balances, the domain equations and also the boundary equations implemented. At the end of the chapter, a section of the validation data and the experiment plan are presented. Simulations and results are presented in Chapter 6. Chapter 7 contains the comparison of the different tuning principles, the most promising tuning principle, the accuracy of the model and future work. The manual for tuning the controllers can be found in Appendix D

2

Automatic Control Theory

This chapter will describe the basic of automatic control theory, the PID-controller, process characteristics and process parameters. Followed are the tuning principles examined in the thesis.

2.1 Intro

Automatic control theory is the principle of controlling a process so it behaves in a desired way, e.g. maintain a certain velocity in a vehicle or keeping the temperature in room stable. By understanding the physics of a process, it can be described mathematically as a system, $P(s)$. The system can then be controlled with the use of a reference value r (or SP, set point), to a controller, $C(s)$. The controller calculates a control output u_c (CO) to the process. The process variable (PV) of the process, y , is the observed process value from the control output. This is called an *open-loop* system, $G_{ol}(s) = P(s)C(s)$, see Fig. 2.1. Often, the mathematical model is simplified as the physics is too complex to completely describe the process, which leads to that the PV can differentiate from the SP. By taking the difference of the PV and the SP, one gets an error $e = r - y$. By using the error as an input to a controller, one can minimize the error. This is called a *closed-loop* system, $G_{cl}(s) = \frac{G_{ol}(s)}{1 + G_{ol}(s)}$, as the system takes the feedback into account, see Fig. 2.2 [Hägglund, 2013]

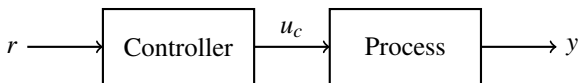


Figure 2.1 Simple open-loop control

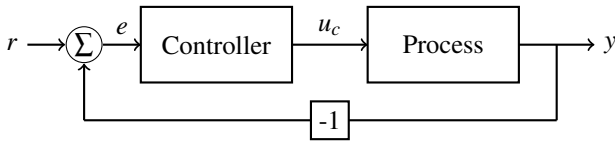


Figure 2.2 Simple closed-loop control

2.2 PID-controller

The PID-controller (abbreviation for *Proportional Integral Derivative*) is one of the simplest form of feedback control for a system. The PID-controller in standard continuous time is shown in (2.1a) and the transfer function in the Laplace domain (2.1b),

$$u(t) = K \left(e(t) + \frac{1}{T_i} \int e(\tau) d\tau + T_d \frac{d}{dt} e(t) \right), \quad (2.1a)$$

$$U(s) = K \left(1 + \frac{1}{T_i s} + T_d s \right). \quad (2.1b)$$

K , T_i and T_d in (2.1a) and (2.1b) are the tuning parameters for the proportional, integral and derivative gain of the controller respectively.

The proportional gain K is a scaling factor of how the output will be affected by the control error.

The integral gain T_i tunes the integral of the control error over time.

The derivative gain T_d tunes the derivative of the control error which calculates in what direction it is moving.

It is common to exclude the derivative part of the PID-controller to achieve a PI-controller.

2.3 Process characteristics

In order for the PID-controller to work efficiently and with desired results, the parameters K , T_i and T_d need to be adjusted correctly for the system. There are several ways to tune a PID-controller. One needs to take into account what kind of process it is. How fast is it, are there any time delays, does it need to handle load disturbances well, does a mathematical model exist, or are there limitations on the control output? These formulations are among a few that can lay ground for what kind of tuning principle that could be efficient. In the following sections Sec 2.4, Sec 2.5 and Sec 2.6, the fundamental principles of a few tuning principles will be explained, as they will be evaluated in the project.

Process parameters

Many tuning principle algorithms rely on the process parameters; the process gain K_p , the time constant T and the time delay L . If the transfer function of the process is known, one can simulate the system and use the *final value theorem* and other methods to derive these parameters. If the transfer function is unknown, these three parameters can be approximated by setting the controller into manual mode and performing a step change of the control output. K_p can then be calculated with the following equation (2.2), where ΔPV and ΔCO are in %. An example of a step response on a *First Order system with Time Delay* (FOTD) (2.3) can be seen in Fig. 2.3.

$$K_p = \frac{\Delta PV}{\Delta CO} \quad (2.2)$$

$$P(s) = \frac{K_p}{Ts + 1} e^{-Ls} \quad (2.3)$$

The time constant of the process, T , is the amount of time it takes for the process to reach 63% of its final value after a change in CO, seen in Fig. 2.3. It also shows the effect of a time delay L , the amount of time before the process reacts to a change in CO. If the system is of higher order, the dominating time constant can be calculated by finding the value where the tangent of the largest derivative of PV after a control output change crosses the original PV value. The difference between that point and 63% ΔPV is the dominating T , an example is shown in Fig. 2.4. If several step responses with different amplitudes on the control output are used, choose the largest K_p and longest T .

Integral Absolute Error

Integral Absolute Error (IAE) is a measure to create a benchmark for different control parameters. It is the sum of the absolute value of the error during recovery time of a load disturbance.

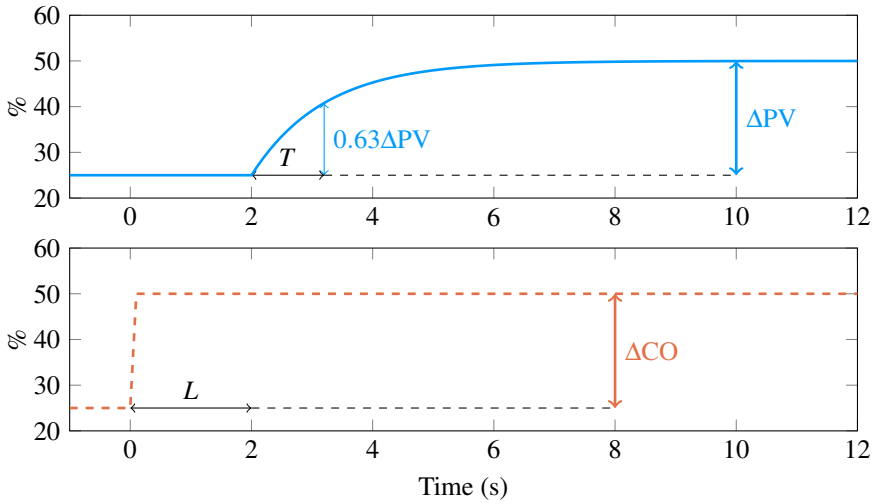


Figure 2.3 Step response on a FOTD (2.3) with time delay $L = 2$. The solid line is the PV and the dashed line is the CO. The time constant $T = 1.2$ s can be calculated by observing the amount of time it requires for the system to reach 63 % of its final output after the time delay L has passed.

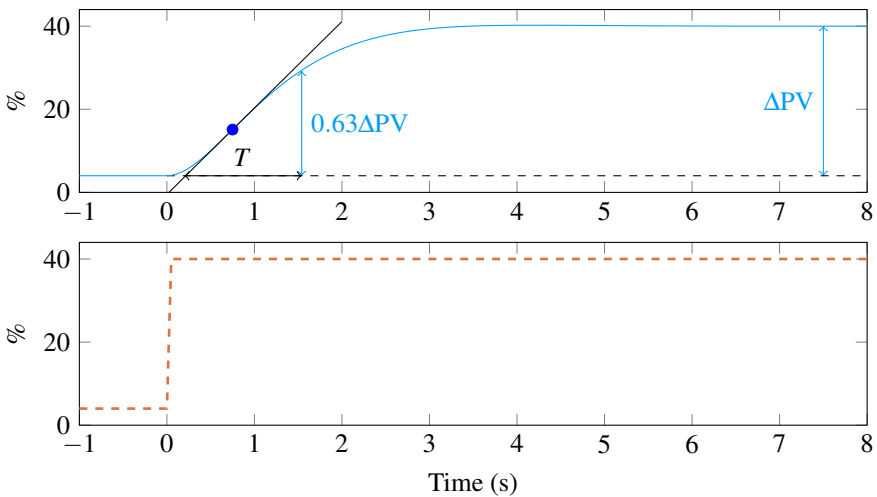


Figure 2.4 Step response on a second order system. The time constant T can be approximated by observing the amount of time it requires for the system to reach 63 % of the final output from the intersection of the tangent at the highest derivative in the slope.

2.4 Approximate M-constrained Integral Gain Optimization (AMIGO)

The AMIGO-tuning principles was developed by Tore Hägglund and Karl J. Åström. It is a tuning principles that focuses on load disturbances, but also have a robustness constraint [Åström and Hägglund, 2006].

With a joint sensitivity of $M = 1.4$ (sensitivity M_s equals complementary sensitivity M_t), the following AMIGO tuning formula for a PI controller is given

$$K = \frac{0.15}{K_p} + \left(0.35 - \frac{LT}{(L+T)^2}\right) \frac{T}{K_p L} \quad (2.4a)$$

$$T_i = 0.35L + \frac{13LT^2}{T^2 + 12LT + 7L^2}. \quad (2.4b)$$

Suggested AMIGO tuning principles for PID are,

$$K = \frac{1}{K_p} \left(0.2 + 0.45 \frac{T}{L}\right) \quad (2.5a)$$

$$T_i = \frac{0.4L + 0.8T}{L + 0.1T} L \quad (2.5b)$$

$$T_d = \frac{0.5LT}{0.3L + T} \quad (2.5c)$$

Fig. 2.5 shows an AMIGO tuned controller for a FOTD (2.3) with varying time delays.

The drawback of AMIGO tuning is the dependency of the time delay L in the tuning rules, with a sensitivity of $M = 1.4$. For processes with very short or no time delay, the CO might exceed its allowed limitations, see Fig. 2.5 for $L = 0.1$ where the CO is far over 100 %.

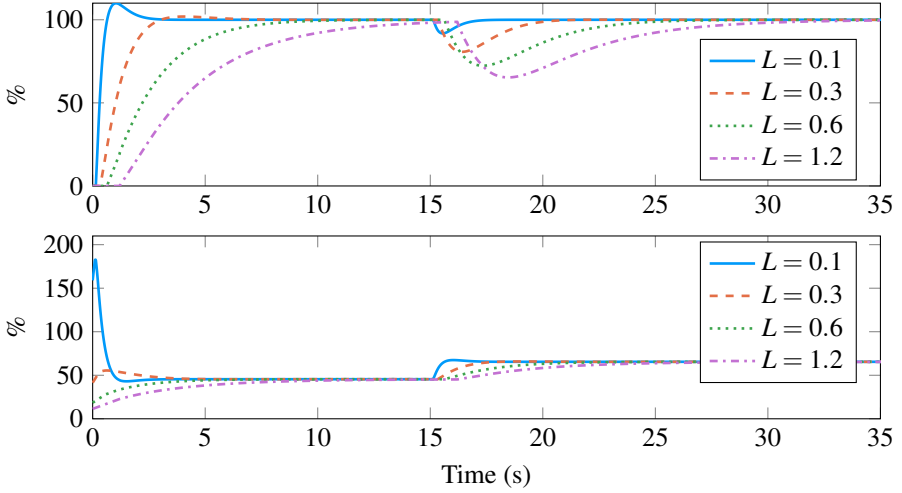


Figure 2.5 Step response and load disturbance on the closed-loop system of a FOTD (2.3) with an AMIGO tuned controller and with varying time delays. The upper figure is the PV and the lower figure is the CO. Note the overshoot for $L = 0.1$ s & $L = 0.3$ s and the attenuation of a load disturbance for the various choice of L at 15 s. Also note the rapid change in the CO for $L = 0.1$ s.

2.5 Lambda Tuning

The Lambda tuning method is a method that cancels out a process pole and with correctly chosen parameters make the step response time of a SP change to λ . It is often used in the process industry [Åström and Hägglund, 2006].

For a PI controller, the process is modeled as a FOTD system, the controller with $T_i = T$ and by approximating the time delay with Taylor series expansion, the loop transfer function becomes

$$G_l(s) = P(s)C(s) = \frac{KK_p}{sT} e^{-sL} \approx \frac{KK_p(1-sL)}{sT}, \quad (2.6)$$

leading to the characteristic equation of the closed loop system

$$s(T - K_pKL) + K_pK = 0. \quad (2.7)$$

By placing the closed-loop pole on the left hand plane at $s = -1/\lambda$, leads to the simple tuning rule

$$K = \frac{1}{K_p} \frac{T}{L + \lambda}. \quad (2.8a)$$

$$T_i = T \quad (2.8b)$$

λ is the closed-loop time constant. A common rule of thumb is to choose $\lambda = 3T$ for a robust controller and $\lambda = T$ for an aggressive controller.

Fig. 2.6 shows the closed-loop step response with a load disturbance on a FOTD system with a lambda tuned controller with varying time delays L and choice of λ .

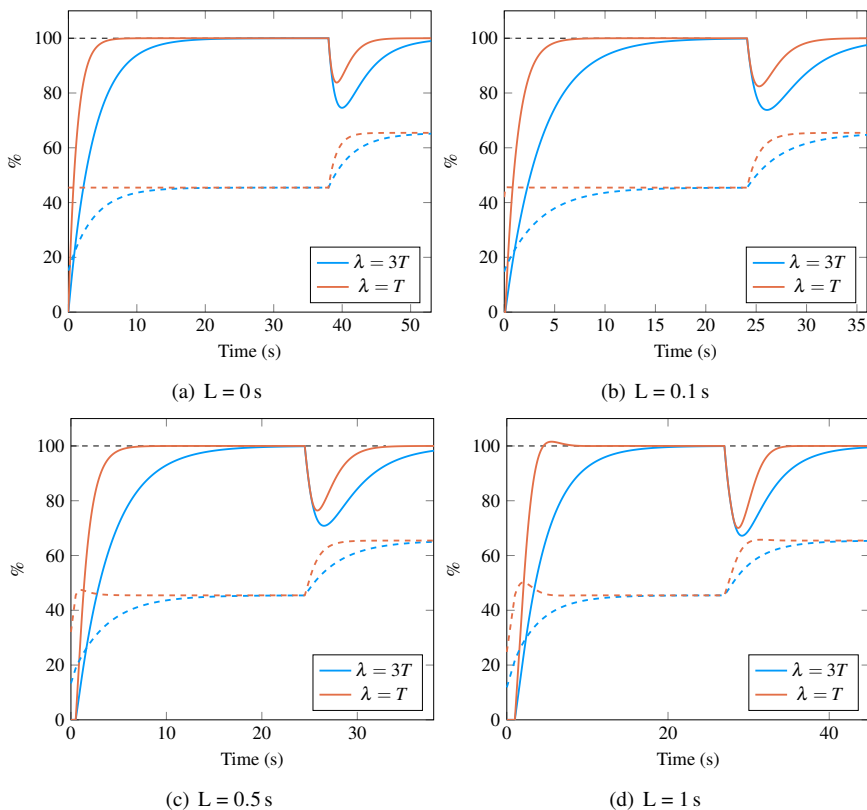


Figure 2.6 Closed-loop step response with a load disturbance on a FOTD system with various choice of L , showing the difference of the rule of thumb for choice of λ . The dashed lines are the control signal to the process. The system recovers faster with the aggressive choice of λ , but overshoots for larger L .

When λ is proportional to T , the integral gain is thus small for large T . The response to load disturbances may be poor for lag-dominated processes [Åström and Hägglund, 2006].

2.6 Skogestad's Internal Model controller (SIMC)

SIMC is a version of the Internal Model Control (IMC) tuning method which avoids the drawback of poor response of load disturbances if the canceled poles are slow in comparison to the dominant poles [Åström and Häggglund, 2006].

SIMC requires that the closed-loop system is on the following form,

$$G_{yy,sp} = \frac{1}{1 + sT_{cl}} e^{-sL}, \quad (2.9)$$

where T_{cl} is the closed-loop time constant. With a FOTD process, the following controller is achieved,

$$C = \frac{1}{P} \frac{G_{yy,sp}}{1 - G_{yy,sp}} = \frac{1 + sT}{K_p(1 + sT_{cl} - e^{-sL})} \approx \frac{1 + sT}{sK_p(T_{cl} + L)}, \quad (2.10)$$

where the time delay has been approximated with Taylor series expansion. The choice of $T_{cl} = L$ is recommended [Åström and Häggglund, 2006]. The tuning rule for PI is

$$K = \frac{T}{2K_pL} \quad (2.11a)$$

$$T_i = \min(T, 8L). \quad (2.11b)$$

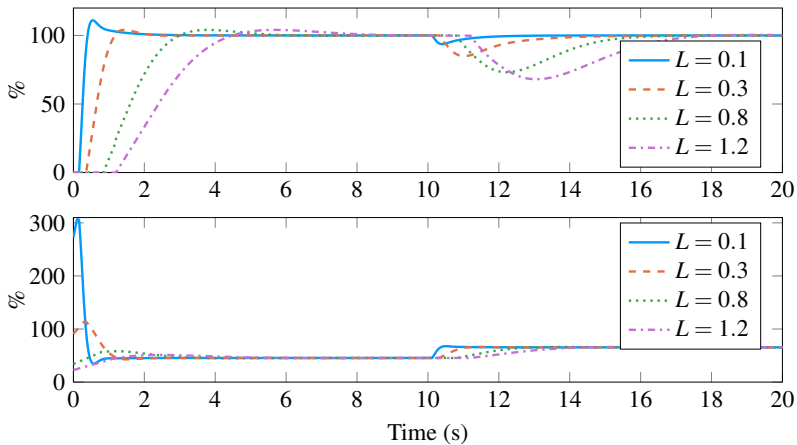


Figure 2.7 Step response and load disturbance on a FOTD with a SIMC tuned controller with varying time delays. The upper figure is the PV and the lower figure is the CO. Note the consistent overshoot in the PV and that the CO for FOTD with less dead time have rapid changes in the signal.

3

Thermodynamics

The chapter covers the basic theory of heat transfer, combustion and numerical methods used to create the mathematical model of the furnace.

3.1 Heat transfer

Heat energy resides within all objects and is generated from the movements of the atoms within an object. Heat is always transferred from a warmer medium to a colder medium. There are three ways that heat can be transferred between two mediums; conduction, convection and thermal radiation [Sunden, 2012].

Conduction

Heat conduction is when heat is transferred through a solid object or fluid at rest. The heat flux is as follows [Sunden, 2012],

$$q = -\lambda \frac{\partial T}{\partial n}, \quad (3.1)$$

q is the heat flux W/m^2 , λ is the thermal conductivity $W/(mK)$ and $\partial T/\partial n$ is the temperature gradient in the direction of the surface normal vector.

The following equation (3.2) is the general heat conduction equation for isotropic materials,

$$\frac{\partial T}{\partial t} = \frac{\lambda}{\rho C_p} \nabla^2 T + \frac{Q'}{\rho C_p} = \frac{\lambda}{\rho C_p} \left(\frac{\partial^2 T}{\partial x^2} + \frac{\partial^2 T}{\partial y^2} + \frac{\partial^2 T}{\partial z^2} \right) + \frac{Q'}{\rho C_p} \quad (3.2)$$

where t is time, ρ is density kg/m^3 , C_p is specific heat capacity $J/(kgK)$ and Q' is internally generated heat.

Convection

Thermal convection is due to molecular movement in fluids (liquids and gases). Convection occurs with fluids in contact with solid bodies. There are mainly two

types of convection, *natural convection* or *free convection* as it occurs naturally for fluids in environments. The molecular movement is created by the difference in density of the fluid as some molecules are subjected to heat transfer and thus change density, causing movement. It is a slow heat transfer which is often neglected in favor of *forced convection* which is caused by driving the fluid with e.g. pumps or fans causing a change in pressure and thereby movement.

Thermal Radiation

Thermal radiation is electromagnetic radiation in mainly the infrared spectra and ranges from $10^{-1} \mu\text{m}$ to $10^2 \mu\text{m}$ [Sunden, 2012]. Compared to the two other heat transfers mentioned before, two mediums of different temperature does not need to be in contact with each other for heat transfer through radiation to occur. The heat is transferred through photons which travel at the speed of light carrying the energy. The frequency ν and the wavelength λ of the photons determine the part of the spectra for the photon. "The propagation of the thermal radiation takes place in form of discrete quanta, where each quanta has energy as

$$E_{\text{quanta}} = h\nu \quad (3.3)$$

where h is Plank's constant with the value $h = 6.625 \times 10^{-34} \text{ Js}$ [Sunden, 2012].

When radiant energy from a warmer medium comes into contact with the surface of a colder medium it can either be reflected ρ , absorbed α , transmitted τ through the medium or a combination of those. The relation between the states outcome is the following

$$\rho + \alpha + \tau = 1 \quad (3.4)$$

Solid objects do not transmit any of the incident radiation, thus $\tau = 0$.

The Stefan-Boltzmann law (3.5) describes the radiation emitted from a black body,

$$E_B = \sigma T^4, \quad (3.5)$$

where $\sigma = 5.67 \times 10^{-8} \text{ W}/(\text{m}^2 \text{ K}^4)$ is Stefan-Boltzmann constant, E_B is the energy from a black body and T is temperature in K. In reality, there are no real perfect black bodies and thus an emission variable ϵ is added to the (3.5), yielding the gray body,

$$E_G = \sigma \epsilon T^4. \quad (3.6)$$

With the use of the *net-radiation method*, developed by Poljak [Siegel and Howell, 2002], one is able to calculate the average radiation transfer between sides in an enclosure with the use of the following equations (3.7) and (3.8),

$$\frac{Q_k}{A_k} = q_k = \frac{\epsilon_k}{1 - \epsilon_k} (E_{B,k} - J_k) \quad (3.7)$$

$$\frac{Q_k}{A_k} = q_k = J_k - \sum_{j=1}^N F_{k-j} J_j, \quad (3.8)$$

where q_k is heat flux W/m^2 , Q_k is heat transfer rate W , A_k is area m^2 , J_k is the absorbed energy through thermal radiation W/m^2 for the side with index k and F_{k-j} is the view factor, explained in Sec 3.2.

By solving (3.7) for J_k and substituting it into (3.8), the following equation is achieved,

$$\sum_{j=1}^N \left(\frac{\delta_{kj}}{\epsilon_j} - F_{k-j} \frac{1 - \epsilon_j}{\epsilon_j} \right) q_j = \sigma T_k^4 - \sum_{j=1}^N F_{k-j} \sigma T_j^4 \quad (3.9)$$

$$\delta_{kj} = \begin{cases} 1, & \text{if } j = k \\ 0, & \text{otherwise.} \end{cases}$$

With known temperature at a specific point in time, the net heat flux for every side in the enclosure due to thermal radiation can be calculated.

[Siegel and Howell, 2002].

3.2 View factor

View factor is the amount of radiation that leaves surface A and intercepts surface B, denoted $F_{A \rightarrow B}$. The sum of view factors leaving a surface is always equal to one.

The view factor from a general surface A_1 to another general surface A_2 is given by equation (3.10) and Fig. 3.1

$$F_{1 \rightarrow 2} = \frac{1}{A_1} \int_{A_1} \int_{A_2} \frac{\cos \theta_1 \cos \theta_2}{\pi r_{12}^2} dA_1 dA_2. \quad (3.10)$$

View factors have the *Superposition* rule and the *Reciprocity* rule

$$F_{1 \rightarrow (2,3)} = F_{1 \rightarrow 2} + F_{1 \rightarrow 3} \quad A_A F_{A \rightarrow B} = A_B F_{B \rightarrow A}$$

As (3.10) is quite complex to calculate, equations for some common geometrical shapes and constellations can be found in Appendix A.

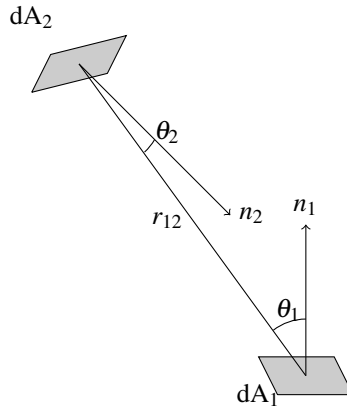


Figure 3.1 Two differential areas in arbitrary configuration [*Radiative view factors*].

3.3 Combustion

Höganäs uses natural gas as fuel in order to heat up the furnace. From the combustion, fumes are generated. As convection between the fumes and the walls occur, the temperature of the fumes, T_g , has to be calculated, which can be done with the following relation (3.11). Note that only a percentage of the energy converted from the combustion of the natural gas is transmitted by radiation, the rest heats up the fumes, thus $P_{gas} < P_{total}$,

$$P_{gas} = \dot{m}C_pT_g, \quad (3.11)$$

where C_p is the specific heat capacity of the gas mixture that Höganäs uses and \dot{m} is the amount of fumes created Nm^3/h , calculated with (3.12),

$$\dot{m} = \frac{P_{total}}{H_i}g, \quad (3.12)$$

H_i is the heating value and g is the factor of fumes generated from the amount of fuel $\text{Nm}^3/(\text{Nm}^3)$ applied [Nilsson, 2011]. For further details, see Appendix B.

3.4 Stepping through time

The general heat equation (3.2) is a *partial difference equation* (PDE). PDE are defined on a domain Ω (surface for 2D) and around the domain, it is surrounded by boundaries Γ (edges for 2D). One way to solve the PDE numerically is to use the *Finite Element Method* (FEM). It is to divide the domain into a mesh of nodes. The PDE is discretized over the nodes and the heat transfer is calculated between the

nodes. PDEs require boundary conditions for the nodes at the boundary and initial conditions for the nodes in the domain. The initial condition is the initial state of the nodes at the beginning of the solution and the boundary conditions describe how the domain interacts with other mediums or domains. There are mainly two different kind of boundary conditions. The *Dirichlet-condition* where the value of the boundary is known and the *Neumann-condition* which describes the value of the derivative at the boundary [Sauer, 2012].

For a simple unsteady heat transfer function (3.2) in one Cartesian dimension with no internally generated heat,

$$\frac{\partial T(x,t)}{\partial t} = \alpha \frac{\partial T(x,t)}{\partial x^2} \quad (3.13)$$

where $\alpha = \frac{\lambda}{\rho C_p}$. The temperature is set as $T(x_n, t_k) = T_n^k$, where $t_k = k\Delta t$, $\Delta t = 1/K$, $k = 0, 1, \dots, K$ and $x_n = n\Delta x$ where Δx is the distance between the nodes.

The PDE is then differentiated in time and in the Cartesian coordinate. The following are differentiation with the *Forward Difference Method* (FDM).

$$\frac{\partial T}{\partial t} \approx \frac{T_n^{k+1} - T_n^k}{\Delta t} \quad \text{Forward difference} \quad (3.14a)$$

$$\frac{\partial T}{\partial x} \approx \frac{T_{n+1}^k - T_{n-1}^k}{2\Delta x} \quad \text{Central difference of first order} \quad (3.14b)$$

$$\frac{\partial^2 T}{\partial x^2} \approx \frac{T_{n+1}^k + T_{n-1}^k - 2T_n^k}{(\Delta x)^2} \quad \text{Central difference of second order} \quad (3.14c)$$

By inserting (3.14a) and (3.14c) into (3.13) and moving all temperatures at the current time step T^k to the right hand and side of the equation and denoting $\sigma = \alpha \frac{\Delta t}{(\Delta x)^2}$, the following equation is achieved (3.15),

$$T_n^{k+1} = \sigma T_{n-1}^k + (1 - 2\sigma)T_n^k + \sigma T_{n+1}^k, \quad (3.15)$$

with the boundary and initial conditions

$$T(0,t) = f(t) \quad T(N,t) = g(t) \quad T(x,0) = h(x).$$

Eq. (3.15) can be represented in matrix form

$$\begin{bmatrix} T_0 \\ T_1 \\ T_2 \\ \vdots \\ T_{N-1} \\ T_N \end{bmatrix}^{t+1} = \begin{bmatrix} 1 & 0 & \dots & 0 & \dots & 0 \\ \sigma & (1-2\sigma) & \sigma & 0 & \dots & 0 \\ 0 & \sigma & (1-2\sigma) & \sigma & 0 & 0 \\ \vdots & & & \ddots & & \\ 0 & \dots & 0 & \sigma & (1-2\sigma) & \sigma \\ 0 & & \dots & & 0 & 1 \end{bmatrix} \begin{bmatrix} f(t) \\ T_1 \\ T_2 \\ \vdots \\ T_{N-1} \\ g(t) \end{bmatrix}^t \quad (3.16)$$

which can be solved with e.g. Gaussian elimination [Sauer, 2012].

Since FDM is explicit, it is an unstable method and must fulfill the stability criteria

$$\sigma < \frac{1}{2}.$$

There are other differentiation method such as the backwards difference method and the Crank-Nicolson method. The Crank-Nicolson method is both implicit and explicit, but more complex to implement. Backwards difference is implicit, but slower. FDM is easier to implement and fast [Sauer, 2012], as long as the stability criteria is fulfilled.

3.5 Exponential smoothing

If measured data contains noise or rapid changes, that is unsatisfactory to observe, one can smooth the data by the use of basic exponential smoothing (3.17),

$$s_t = \alpha x_t + (1 - \alpha)s_{t-1} \quad (3.17)$$

where s_t is the smoothed data, x_t is the measured data and α is the smoothing factor, $0 < \alpha < 1$. The smoothing factor can be chosen to achieve a specific time constant on the filter, described as the following

$$\alpha = 1 - e^{-\frac{\Delta t}{T}}$$

$$\alpha \approx \frac{\Delta t}{T}$$

if the sampling time is fast, comparing to the time constant.

4

The Process

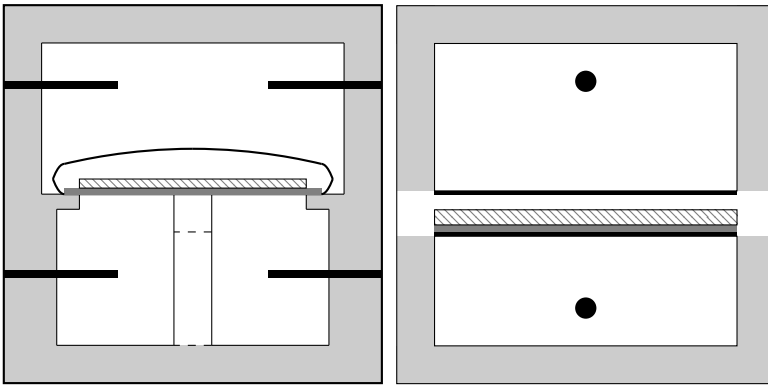
This chapter explains how the process works starting from when the powder is added to the process into the heating Sec 4.1, to exiting from the cooling Sec 4.2. As the model will simulate the heating, it is more thoroughly explained than the cooling.

4.1 The Heating

The heating consists of an upper and lower combustion area, separated by the muffle. The iron powder is added evenly onto the conveyor belt in front of the furnace. The powder is then transported on the belt through the furnace inside of the muffle which separates the powder from being in contact with the fuel and the fumes in the combustion areas. The muffles shape is arched and ribbed and its weight is supported on its sides and by a pillar beneath with vaults, see Fig. 4.1(a) for an illustration.

Each combustion area is divided into several temperature zones. The furnace that has been modeled, BU28, has in total eight temperature zones above the muffle and another eight zones beneath the muffle, see Fig. 4.2. The length of these zones varies, with shorter zones at the beginning and at the end of the process to longer zones in the middle. The heat transfer loss is larger in the beginning of the process as the powder has a lower temperature in comparison with the temperature in the first zones. There are several burners evenly distanced alongside the furnace in each temperature zone, with one on every other side (in the bottom zones, the burners flames pass through the vaults). Between the burners, there is a shielded temperature sensor. The burners ignites natural gas which heats up the walls and the muffle in the zone through thermal radiation and also by the convection through the fumes.

At the end of the furnace, there is a specific valve for the fumes, which keeps the pressure in the zones below atmosphere pressure, thus preventing fumes to exit the furnace at undesired leakages and harming the personnel. The valve also ensures that the fumes move alongside the furnace, thus decreasing the output of the burners further down in the furnace. The furnace walls are insulated with several



(a) The light gray areas are the insulation of the furnace. The darker gray rectangle is the combustion zone, the thick solid black lines are the conveyor belt and the patterned rectangle is the muffle, the dark grey rectangle is the powder bed. The bent form is the muffle conveyor belt, the upper white rectangle is the upper combustion zone and also the lower combustion zone including the upper combustion zone and the light grey is the insulation of the walls. The burners are merged into a single burner and positioned in the middle of the zone. Note that there is no insulation on the muffles side.

Figure 4.1 Illustration of the cross section of the furnace. Fig. 4.1(a) shows the geometry and Fig. 4.1(b) the simplifications made.

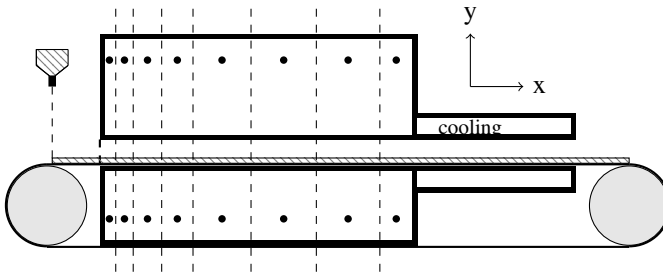


Figure 4.2 Illustration of the cross section alongside the furnace. The heating zones are separated by the dashed lines and the cooling section afterwards by the rectangles. Powder is added onto the conveyor belt and is dropped down into a crusher afterward. The small black circles are the combined burners. Note that the dashed lines only illustrate the zones, in reality there are no barriers separating them.

materials with different physical characteristics, for details see Appendix C. In the muffle, a reduction gas enters from the opposite direction of the powder. As the

powder is heated, it reacts with the reduction gas and is purified. The reduction gas exits through the powder entrance of the muffle where it is ignited, which heats the powder before it enters the muffle.

Outside of the furnace, the natural gas is mixed with air. Once the gas enters the furnace during run-time, it ignites due to the high temperature.

4.2 The Cooling

In the cooling zone, the powder is cooled down by recircling processgas, which in turn is cooled down by water. Once the powder has left the cooling area, it is cool enough to not react with the oxygen in the air [Håkansson and Andersson, 2007].

4.3 Control

The process is controlled with what Höganäs AB calls *rate control* (Sv. taktstyrning). The natural gas burners in the heating zones runs intermittently (on-off). The ratio of on and off is controlled by a PID-controller in each heatzone. The system is sampled at each second and calculates the control signals for the next upcoming 120 s and is updated each second. If the control signal is at 100 %, all burners will be turned on at the same time for 120 s. If a zone has e.g. four burners, at 25 %, these will burn for 30 s. Each burner has an output ~ 116 kW. The system has a security limit at the maximum output of 2.2 MW for the whole furnace. At normal run time, the total output is approximately 1.7 MW.

Each burner has a specific time slot during the 120 s interval when it is possible for it to ignite. First, each zone is iterated, enabling the first burner to be able to ignite. Once all zones have been iterated through, it reiterates, thus allowing the second burner to ignite. This is checked by an AND-grind and a flip-flop. The flip-flop samples every 250 ms and has a real-time clock, thus updating with the time left for the burner to run.

The controllers are implemented with ABB 400-series control units with the controller in standard form (2.1a) and primarily only use the K and T_i parameters.

Höganäs has a start-up sequence for the furnaces since there are limitations and watchdogs controlling the power output of the burners, shutting the system down if the furnace is draining too much power. The system also has a on and off controller, putting the burners on maximum output or turning them off if the PV drifts too far away from the SP. If there is a belt stop, the system will automatically lower the SP for all zones, making the system recover faster when the conveyor belt is running again.

The *Human Machine Interface* (HMI) system samples the value every second, but only logs every ninth second, which sets a constraint on the sampled data gained from the logs.

5

Modeling

This chapter covers how the model was built, simplifications and the numerical setup.

5.1 Intro

One can either build a model of a process mathematically by using the laws of physics or by system identification techniques. There are several reasons why one might want to build up a mathematical model of a process. It could either be too expensive to run experiments on the process for a full analysis, as material would go to waste (cost) or the amount of time that the process is unusable from normal drift (cost). It could also be too dangerous to conduct the experiments e.g. a nuclear power plant in Chernobyl or the process does not simply exist yet.

When modeling, simplifications have to be done. If one were to try to model the complete physical behavior of the process, it would become computationally heavy and it might even then not catch every detail of how the process works. In order to validate if the model is accurate enough to simulate the real process, one can compare data from the real process (if it exists) with the simulated data by inserting the same control signal.

The purpose of this modeling was to catch the major dynamics of the process.

5.2 Simplifications

Several simplifications of the process were done during the modeling, many based on an earlier thesis where they made a static model [Håkansson and Andersson, 2007]. The simplifications were made in order to make the model easier to implement and because of lack of real data that weren't available.

The major simplification that was made was the geometry of the furnace. A simple illustration can be seen in Fig. 4.1(a) and the simplifications made in Fig. 4.1(b). The burners were combined into a single one, which will lead to that heat from the

combined burner will have a greater impact on the nodes on the muffle in the middle of a zone, compared to the real one were they are spread out and are turned on at different time intervals. The thermal radiation was simplified so the wall, muffle and the burner only interact with each other in a zone. In the first two upper temperature zones, there is an additional booster burner. They were simplified as the other burners with natural gas as fuel, as a bias on the CO. As the fuel is ignited, some of the energy is turned into thermal radiation, while some heats up the gas. This ratio and the behavior is unknown, but is approximated to 20 % that turns into thermal radiation [Garner, 1948]. The thermal radiation from a node to another were uniformly distributed on the node. The fumes that are created from the combustion were simplified due to lack of knowledge of Navier-Stokes equations. The fumes generated does not radiate and are simplified as a homogeneous gas in each zone, meaning that the gas temperature is the same everywhere in a zone. Since the pressure in the furnace is controlled and kept at a stable level, the movement of the fumes were simplified so only the generated fumes travel to the next zone. In the real process, it is possible for the fumes to move from the upper combustion zones to the lower and one can see in the data from a step response that also both adjacent zones are affected. The simplification will lead to that earlier zones aren't affected by a change of CO later in the furnace. Less heat is also transferred when solving the thermal radiation equation for enclosures (3.8), as only the nodes in the same zone are included in the equation due to complexity, leading to heat loss and not equivalent to emitted and absorbed. The width of the combustion zone were set as the same width as the muffle.

The muffles shape would be difficult to model as it was arched and ribbed, so it was simplified as a plane and with no insulation on the sides. This should lead to that less heat is transferred to the muffle as heat otherwise could be transferred from the sides as well through thermal radiation and convection. The pillar supporting the muffle on the sides were removed and also the support beneath. The equation used for solving the thermal radiation requires that it is an enclosure, where all sides exchange heat with each other. As the sides were removed, some heat is lost from the thermal radiation, thus the powder will have a lower temperature as less heat is transferred.

Inside the muffle, the conveyor belt and the powder received the same width as the muffle, where the width of the powder bed is actually smaller than the belt. Heat were set so it only travels in two directions in the powder, along the direction of the conveyor belt and towards the combustion zones. The inlet temperature of the powder and the conveyor were set to a constant based on tests made by Höganäs to determine the temperature in the powder [Håkansson and Andersson, 2007]. Due to the outlet of the muffle, the powder starts to cool at the end of the furnace, approximately 0.5 m, but was ignored.

The reduction gas that enters the muffle from the opposite direction of the powder is ignored in the model. In reality, the gas interacts with both the muffle and the powder through convection.

As the temperature of the powder rises, the annealing process starts to take place. As the powder becomes more purified, its physical properties changes and some minor heat is generated due to the reaction. This was also ignored as the generated heat is minor in comparison with the other heat transfers.

The thickness of the conveyor belt is set as a constant, but actually changes over time, getting thinner due to the reheating and stretching of the material.

Many material parameters such as density, specific heat capacity, thermal conductivity and more are dependent on the temperature. Due to the thermal radiation, the process is non-linear and as the model were to be modeled around the process normal SP, these variables were set to constants. Some constants are also simplified as the materials property at 0 °C or room temperature, due to lack of data of the values around the SP. These simplifications will remove some of the dynamics of the system. Due to lack of data for some of the insulation materials in the combustion zones, an initial guess of the properties were made based on similar materials.

Fig. 5.1 is a representation the domains and boundaries of a cross segment of the furnace, as Fig. 4.1(b).

Γ_{1b}	Γ_{1a} Ω_1	Γ_{1c}	Upper combustion zone
	Γ_2		Muffle top
	Γ_3		
Γ_5	Γ_4 Ω_2	Γ_6	Powder bed
	Γ_7		
Γ_9	Γ_8 Ω_3	Γ_{10}	Conveyor belt
	Γ_{11}		
	Γ_{12}		Muffle bottom
	Γ_{13}		
Γ_{14b}	Ω_4 Γ_{14a}	Γ_{14c}	Lower combustion zone

Figure 5.1 Energy balance of a cross section. Ω_i are domains and Γ_j are boundaries. Note that

5.3 Disturbances

The process is quite stable during run time and seldom turned off. The conveyor belt is changed at certain intervals and during that time, a belt stop occurs. When a belt stop occurs, the speed of the conveyor belt is set to zero and the SP for the heating zones are lowered. This is due to less heat transfer in the furnace as no new "cool" powder enters. Once the conveyor belts speed is returned to its normal state, the SP are restored. It is these belt stops that cause the major load disturbance on the process. A belt stop can also occur due to other reasons not directly connected to the furnace e.g. a container further down the whole process line is full and can't accept more powder or an engine driving the crushers catches on fire.

5.4 Modeling process

The modeling started with the powder bed as a module in the lateral direction (y-direction, see Fig. 4.2). Then in the horizontal (x-direction) along the furnace in the direction of the conveyor belts movement.

Then the module was extended with the boundary conditions for the inlet and outlet in the horizontal direction. The next step was working downwards with the conveyor belt and the muffle bottom, afterwards the radiation from the muffle top to the powder. After that, the radiation heat transfer from the walls to the muffles top and bottom. The module for the combustion area was extended with the burners and the insulation of the combustion areas. Lastly the fumes and convection in combustion zones was added.

Powder bed

In the powder bed, heat is transferred through conduction from the conveyor belt and by thermal radiation from the muffle.

The energy balances in the powder bed domain Ω_2 can altogether be modeled with (5.1).

$$\rho_p C_{p,p} \frac{\partial T}{\partial t} = \nabla(\lambda_p \nabla T) - \bar{\mathbf{u}} \rho_p C_{p,p} \nabla T \quad (5.1)$$

$C_{p,p}$ is the specific heat capacity for the powder, ρ_p is the density of the powder and λ_p is the thermal conductivity of the powder. The conveyor belt is only moving in one direction through the furnace, thus $\bar{\mathbf{u}} = \mathbf{u}_x$. Heat is mostly transferred vertically and horizontally, thus yielding the following for the heat transfer in the powder bed,

$$\rho_p C_{p,p} \frac{\partial T}{\partial t} = \lambda_p \left(\frac{\partial^2 T}{\partial x^2} + \frac{\partial^2 T}{\partial y^2} \right) - \mathbf{u}_x \rho_p C_{p,p} \frac{\partial T}{\partial x}. \quad (5.2)$$

The powder bed were discretized using FDM (3.14). The temperature of the incoming powder bed at boundary Γ_5 is assumed to be known and constant T_{in} ,

therefore the Dirichlet-condition. On the upper boundary Γ_4 and lower boundary Γ_7 the powder is mostly affected by the heat transfer from the thermal radiation and conduction, thus the Neumann-condition. The derivative of the heat transfer for the outgoing powder at the boundary Γ_6 is assumed to be zero, yielding the following boundary conditions with the initial condition,

$$\begin{aligned} T_{1,j}^t &= T_{in} & T_{n_y,j}^t &= T_{n_y-1,j}^t & T_{i,1}^t &= \lambda_p \frac{\partial T}{\partial y} + q_{m,rad} \\ T_{i,n_x}^t &= \lambda_p \frac{\partial T}{\partial y} + q_{cp} & T_{i,j}^0 &= T_0(i, j) \end{aligned}$$

where index i, j are in the vertical and horizontal direction with the lower limit 1 and upper limit n . $q_{m,rad}$ is the thermal radiation heat flux between the muffle and powder and q_{cp} is the heat transferred at the boundary between the powder and conveyor domain,

$$q_{cp} = k_{cp}(T_{\Gamma_8} - T_{\Gamma_7}) \quad (5.3)$$

$$k_{cp} = \left(\frac{\Delta y_{\Omega_2}/2}{\lambda_p} + \frac{1}{k_{cont,cp}} + \frac{\Delta y_{\Omega_3}/2}{\lambda_c} \right)^{-1} \quad (5.4)$$

where T_{Γ_8} is the temperature at the boundary Γ_8 , Δy_{Ω_2} is the distance between the nodes in the y-direction of the mesh in domain Ω_2 , $k_{cont,cp}$ is an estimated contact coefficient [Håkansson and Andersson, 2007] and λ_p and λ_c is the thermal conductivity for the powder and the conveyor belt.

Thus, the temperature at the boundaries is updated with

$$\begin{aligned} T_{\Gamma_4}^{t+1} &= T_{\Gamma_4}^t + \frac{\Delta t}{\rho_p C_{p,p} \Delta y / 2} \left(q_{m,rad} - \lambda_p \frac{(T_{i,1}^t - T_{i,2}^t)}{\Delta y} \right) \\ T_{\Gamma_7}^{t+1} &= T_{\Gamma_7}^t + \frac{\Delta t}{\rho_p C_{p,p} \Delta y / 2} \left(q_{cp} - \lambda_p \frac{T_{i,n_y}^t - T_{i,n_y-1}^t}{\Delta y} \right) \end{aligned}$$

Conveyor belt

In the conveyor belt, heat is transferred through conduction from the powder and from the muffle bottom.

The energy balances in the conveyor is very similar to the powder bed,

$$\rho_c C_{p,c} \frac{\partial T}{\partial t} = \lambda_c \left(\frac{\partial^2 T}{\partial x^2} + \frac{\partial^2 T}{\partial y^2} \right) - \mathbf{u}_c \rho_c C_{p,c} \frac{\partial T}{\partial x}. \quad (5.5)$$

$C_{p,c}$ is the specific heat capacity for the belt, ρ_c is the density of the belt and λ_c is the thermal conductivity of the belt.

The conveyor belt was discretized as the powder bed, with a different choice of n_y .

The temperature of the incoming conveyor belt at boundary Γ_{10} is assumed to be known and constant, therefore the Dirichlet-condition. On the upper Γ_9 and lower Γ_{12} boundary the conveyor belt is mostly affected by conduction, thus the Neumann-condition. The derivative of the heat transfer for the outgoing belt at the boundary Γ_{11} is assumed to be zero, yielding the following boundary conditions with the initial condition,

$$\begin{aligned} T_{1,j}^t &= T_{in} & T_{n_y,j}^t &= T_{n_y-1,j}^t & T_{i,1}^t &= \lambda_c \frac{\partial T}{\partial y} + q_{cp} \\ T_{i,n_x}^t &= \lambda_c \frac{\partial T}{\partial y} + q_{cm} & T_{i,j}^0 &= T_0(i, j) \end{aligned}$$

where q_{cp} is described in the preceding subsection, q_{cm} is the heat transferred between the conveyor belt and the muffle,

$$q_{cm} = k_{cm}(T^{\Gamma_{12}} - T^{\Gamma_{11}}) \quad (5.6)$$

$$k_{cm} = \left(\frac{\Delta y_m / 2}{\lambda_m} + \frac{1}{k_{cont,mc}} + \frac{\Delta y_{\Omega_3} / 2}{\lambda_c} \right)^{-1} \quad (5.7)$$

$k_{cont,mc}$ is the contact coefficient between the muffle bottom and the conveyor belt, λ_m is the thermal conductivity of the muffle and Δy_m is the distance between the two boundaries.

The temperature at the next time step was solved with the same method as for the powder bed.

The muffle

The upper part of the muffle transfers heat through thermal radiation and by convection from the upper combustion zone and through thermal radiation to the powder bed. The lower part of the muffle transfers heat through thermal radiation and by convection from the lower combustion zone and through conduction to the conveyor belt.

Since the geometry of the muffle is simplified, it only interacts at the boundary $\Gamma_2, \Gamma_3, \Gamma_{12}$ and Γ_{13} . Only the heat transfer in the y-direction is considered as no heat is lost to the sides from the simplification. No area on the surface of the the muffle is able to emit or absorb energy from an adjacent area on the same boundary through radiation, therefore $F_{k-k} = 0$. By using Poljaks net-radiation method Sec 3.1, view factor for rectangular planes Appendix A and Fig. 5.2, $q_{m,rad}$ for the boundaries Γ_3 and Γ_4 is obtained.

Each segment affects a total of 37 other segments, as the view factor is very small for the other ones, thus covering more than 165°.

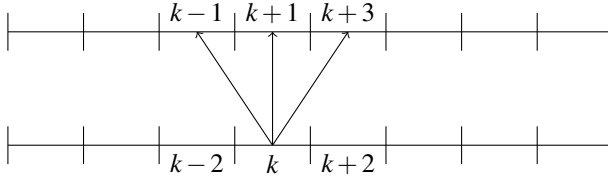


Figure 5.2 Illustration of the numbering and how the heat is emitted from the powder bed to the muffle through radiation.

In the powder bed and the muffle, the nodes didn't have an area, but in order for the heat radiation transfer to occur, the nodes were approximated with an area. Thus there is one area more than actually exist in the system.

The upper and lower part of the muffle only have 2 nodes in the y-direction, one on each boundary. The temperature on the muffle should be almost be the same on its inside and outside.

The heat transfer between these two boundaries is described by

$$T_{\Gamma_3}^{t+1} = T_{\Gamma_3}^t + \frac{\Delta t}{\rho_m C_{p,m} \Delta y / 2} \left(q_{m,rad} + \frac{\lambda_m (T_{\Gamma_2}^t - T_{\Gamma_3}^t)}{\Delta y} \right) \quad (5.8)$$

For the muffle facing the conveyor belt, the heat transfer is described by

$$T_{\Gamma_{12}}^{t+1} = T_{\Gamma_{12}}^t + \frac{\Delta t}{\rho_m C_{p,m} \Delta y / 2} \left(-q_{cm} + \frac{\lambda_m (T_{\Gamma_{12}}^t - T_{\Gamma_{13}}^t)}{\Delta y} \right) \quad (5.9)$$

The combustion zones

In the combustion zones, heat is transferred by conduction through the walls insulation material. Thermal radiation from the inside walls to the muffle and from the burners and also through convection through the fumes.

The thermal radiation heat transfer is calculated the same way as with the muffle (3.8), but with the addition of the burners $J_{b,i}$ and the walls on the side. The burners are placed in the middle of a zone in the x-direction and at a ratio λ of the height on the y-axis,

$$q_{k,rad} = \frac{\varepsilon_k}{1 - \varepsilon_k} (E_{B,k} - J_k) \quad (5.10)$$

$$q_{k,rad} = J_k - \sum_{j=1}^N F_{k-j} J_j - \sum_{i=1}^M F_{i-k} J_{b,i}. \quad (5.11)$$

All nodes on the muffle boundary interacts only with the walls in the same zone and v.v.

As the burners ignite the natural gas, parts of the energy that is released heats up the fumes. The temperature of the gas is calculated through (3.11). The heat flux transferred from the fumes to the walls and muffle is then calculated with

$$q_{k, gas} = \alpha_g (T_k - T_g). \quad (5.12)$$

α_g is the convection term. In the implementation, a mean of the temperature of all the nodes on the muffle are calculated instead of taking each individually. The total heat flux is then subtracted from the energy stored in the gas and a new temperature is recalculated. The fumes are transferred into the next zone and the procedure iterates.

The boundaries Γ_{1a-c} and Γ_{16a-c} are the insulation of the combustion zones. The heat flux from the node within the wall is calculated through (5.13),

$$q_{k, iso} = \frac{\lambda_w (T_L - T_{L-1})}{\Delta x}, \quad (5.13)$$

where λ_w is the thermal conductivity of the material of the wall in contact with the combustion zones, T_L is the node on the wall and T_{L-1} is the node one Δx distance into the wall.

The temperature is then updated with the following equations for the nodes on the walls (5.14) and the muffle (5.15)

$$T_{\Gamma_1}^{t+1} = T_{\Gamma_1}^t + \frac{\Delta t}{\rho_w C_{p,w} \Delta y / 2} (q_{k, tot}) \quad (5.14)$$

$$T_{\Gamma_2}^{t+1} = T_{\Gamma_2}^t + \frac{\Delta t}{\rho_m C_{p,m} \Delta y / 2} \left(q_{k, rad} + q_{k, con} - \frac{\lambda_m (T_{\Gamma_2}^t - T_{\Gamma_3}^t)}{(\Delta y)} \right) \quad (5.15)$$

The temperature is updated with the same equation for boundaries Γ_{15} and Γ_{16} .

Insulation

The insulation of the furnace is modeled with the FDM over two or three domains, sharing boundaries between the materials. The materials have different properties, and were discretized in only one Cartesian coordinate, with the following function,

$$\rho C_p \frac{\partial T}{\partial t} = \lambda \frac{\partial^2 T}{\partial x^2}. \quad (5.16)$$

and a convection term for the boundary outside of the furnace.

Temperature sensor

The temperature sensor dynamic was modeled with basic exponential smoothing to mimic the behavior of the process and its time constant with (3.17). The filter was only applied to the observed data.

5.5 Validation

The experimental plan on how the validation data was gathered and the validation of the furnace.

Experiment plan

The experiment plan for the gathering of validation data was adjusted a couple of times. Below is the final experimental plan after the last data gathering.

1. Verify that the furnace has been in normal operation for the last 8 h and has been stable for the past 4 h. It is stable if there has not been any periodic disturbances or major temperature changes. If not, wait until the system is stable and another 4 h.
2. Put the controller in zone 1, 2 and 3 in both upper and lower combustion areas into manual mode.
 - a) Add 5 % to CO on all zones in manual mode in order to assure that the temperature won't drop below the SP and damage the product.
3. Wait 30 min and observe if the temperature in the zones set to manual are stable. If not, wait until they are stable. Note: The temperature should be a couple °C above the SP.
4. Increase CO in upper combustion zone 2 with 30 %.
5. Wait for the system to stabilize.
6. Wait another 30 min
 - a) Observe if zone 3 in upper combustion area also have stabilized.
 - b) Observe if zone 2 in lower combustion area also have stabilized.
7. Decrease CO in zone 2 in upper combustion area by 30 %.
8. Wait for the system to stabilize.
9. Wait another 30 min
 - a) Observe if zone 3 in upper combustion area have stabilized.
 - b) Observe if zone 2 in lower combustion area have stabilized.
10. Restore the controller in zone 1,2 and 3 in upper and lower combustion area to auto mode.

Experiment plan adjustments The first experiment was conducted with only zone 2 and 3 in the upper combustion zones in manual mode. The test was though redone with zone 2 and 3 in both upper and lower combustion zones i manual mode due to visible effect of the controller output in the lower combustion zone having an impact. The data set were later nullified due to two things. A periodic disturbance with a periodicity that varied between 80 min to 90 min in all zones, see Fig. 5.3. The other reason was the resolution of the AD-converter, which didn't show accurate data, also visible in Fig. 5.3. The resolution was later increased.

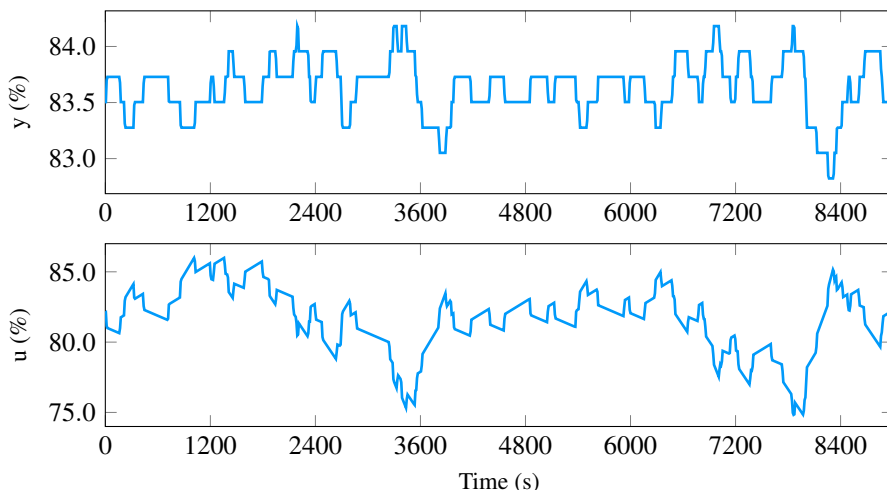


Figure 5.3 Data from the process, zone 1 in upper combustion area . The upper plot is the temperature and lower plot is the control signal. Note the resolution of the measured temperature and also note the periodic disturbance of ≈ 80 min seen in the control signal from approximately 3600 s to 7800 s.

This periodic disturbance was caused by two ratio controllers, both trying to control the air added to the natural gas for the pre-mix. The amplitude of the output of the controller varied for different zones, but were as high as 10 % for Upper Zone 2. As the experiments lasted for at least 60 min, the disturbance from the first zone (not in manual) had an impact on the step response experiment. Some zones exhibit a periodicity of 2 min caused by the placement of the temperature sensor in the zone. These are just examples of how complex the process it is.

Validation data

In Fig. 5.4, two step responses on temperature zone 2 in the upper combustion area are shown. Comparing with the result from the model, seen in Fig. 5.5, the process

gain is similar and also the time constant for the zone.

The previous zones are not affected by the step response, which was mentioned in Sec 5.2. Comparing the model with the process, the temperature in the opposite zone is not affected by the step response.

Fig. 5.6 shows how the process recovers from a belt stop and Fig. 5.7 shows a SP change of the closed-loop system with a PI-controller using the current parameters used at Höganäs. The model behaves in the same way as the process during a SP change for a closed loop system, as there are oscillations in both the temperature and the control signal. It is also important to bear in mind that the recovery from the belt stop is from non stationary while the second figure is stationary before the SP change.

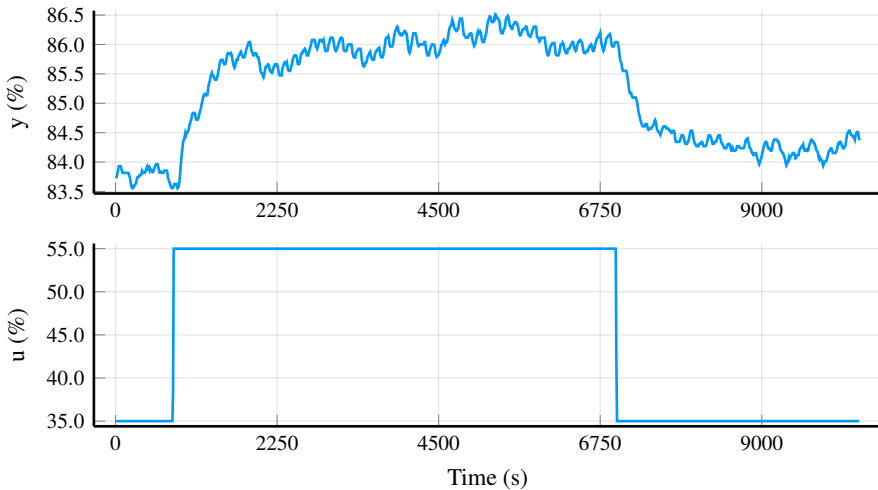


Figure 5.4 Two step responses on temperature zone 2 in upper combustion area on the furnace. Note that the temperature is not the same after the second step response, which might be due to the system not fully stabilized before the first step response. In the second step change, the time delay is close to zero and the time delay in the first step change might be due to noise introduced by the reduction gas burners. In the first step response; $K_p = 0.12$, $T = 486$ s and $L \approx 0$.

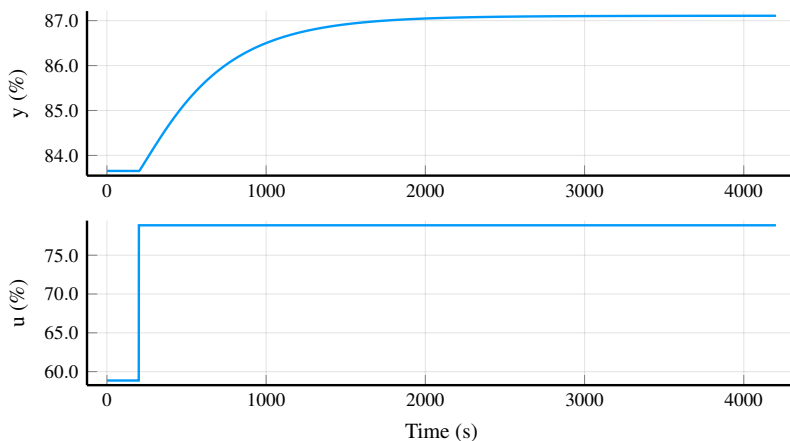


Figure 5.5 Open loop step response at $t = 200$ s on temperature zone 2 in the upper combustion area on the model. $K_p = 0.1727$, $T = 477$ and $L = 0$.

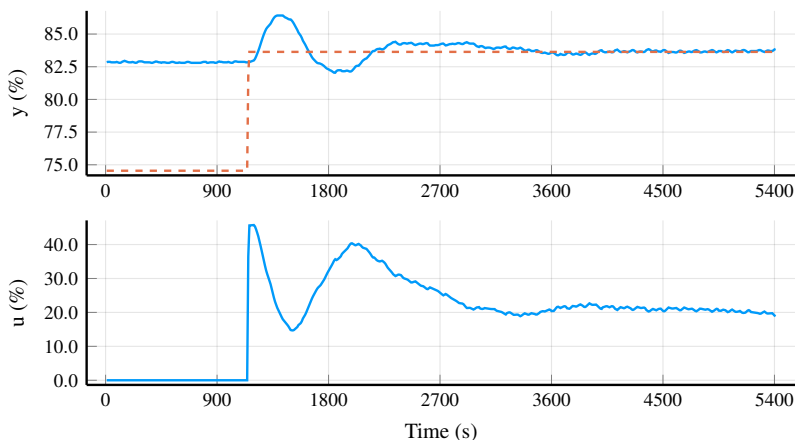


Figure 5.6 Belt stop on the process. The solid line in the upper plot is the measured value of the temperature, the dashed line is the SP and in the lower plot, the solid line is the control signal. As the belt stop occurred, the system lowered the set point for all zones, except for the first upper zone. As the SP is increased again, the conveyor belt starts moving and new cool powder enters the furnace. There is a clear overshoot and oscillation in the measured temperature and control output. This is caused due to the parameter settings of the PI-controller, mainly the time constant which is too short.

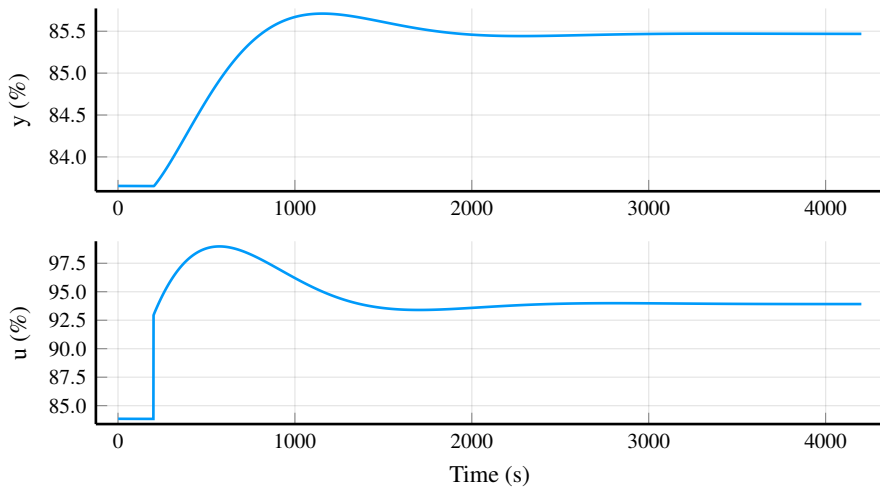


Figure 5.7 Closed loop SP change at $t = 200$ s on temperature zone 2 in the upper combustion area on the model with the controller parameters used at Höganäs.

6

Result

This chapter covers the result from the simulations of the model with the tuning principles examined and the process characteristics of the model. Finally, the chosen tuning principle is presented.

6.1 Simulations

Since the process had no or barely no dead time L , the AMIGO and SIMC tuning principles are not effective as either the proportional gain or the integral gain of the controller would become zero or go to infinity. Therefore, the lambda tuning principle was chosen with different values of λ .

The controller was chosen as a PI-controller, excluding the derivative term of the PID-controller. Step responses were made on each zone to calculate the process gain and time constant for the zone. From them, the controller parameters were calculated using (2.8a) and (2.8b) for each controller. The process parameters are displayed in Table 6.1 and the controller parameters in Table 6.2. Note the different time constants and gain for each zone, which is due to the zones size.

The SP change made on temperature zone 2 in the upper combustion area on the model is shown in Fig. 6.1. The effect on the succeeding zones is presented in Fig. 6.2.

The same were done on temperature zone 4 in upper combustion area, see Fig. 6.3 and Fig. 6.4.

A load disturbance was simulated on the model in temperature zone 2 in upper combustion area, see Fig. 6.5. The corresponding IAE values for the controllers are presented in Table 6.3.

Recommended tuning principle

From the simulations made on the derived model, only the λ -tuning principle were applicable among the three tuning principles examined. Three different settings for the design parameter was simulated and the recommended setting is $\lambda = 2T$.

Table 6.1 Process characteristics for each modeled zone.

Upper								
Zone #	1	2	3	4	5	6	7	8
K_p	0.3165	0.1727	0.1402	0.1179	0.1184	0.1257	0.1232	0.1277
T (s)	446	477	496	497	517	523	519	509
Lower								
Zone #	1	2	3	4	5	6	7	8
K_p	0.6161	0.3774	0.2849	0.2301	0.2293	0.2411	0.2336	0.2372
T (s)	468	507	555	559	597	607	599	578

Table 6.2 Controller gain of the controllers for the model. See Table 6.1 for T_i , as $T_i = T$. The currently used parameters at Höganäs are $K = 5$, $T_i = 180$ s for all zones

Upper Zone #	1	2	3	4	5	6	7	8
$\lambda = 1T$	3.160	5.790	7.135	8.482	8.446	7.957	8.115	7.830
$\lambda = 2T$	1.580	2.895	3.567	4.241	4.223	3.978	4.057	3.915
$\lambda = 3T$	1.053	1.930	2.378	2.827	2.815	2.652	2.705	2.610
Lower Zone #	1	2	3	4	5	6	7	8
$\lambda = 1T$	1.623	2.650	3.510	4.347	4.361	4.148	4.282	4.216
$\lambda = 2T$	0.8116	1.325	1.755	2.173	2.180	2.074	2.141	2.108
$\lambda = 3T$	0.5410	0.8832	1.170	1.449	1.454	1.383	1.427	1.405

Table 6.3 IAE values for a load disturbance on temperature zone 2 in upper combustion area. "Original" are the currently used parameters at Höganäs. The measured values were normalized, see Fig. 6.5.

Controller	IAE
$\lambda = 1T$	8.4217
$\lambda = 2T$	16.4134
$\lambda = 3T$	24.4108
Original	4.6741

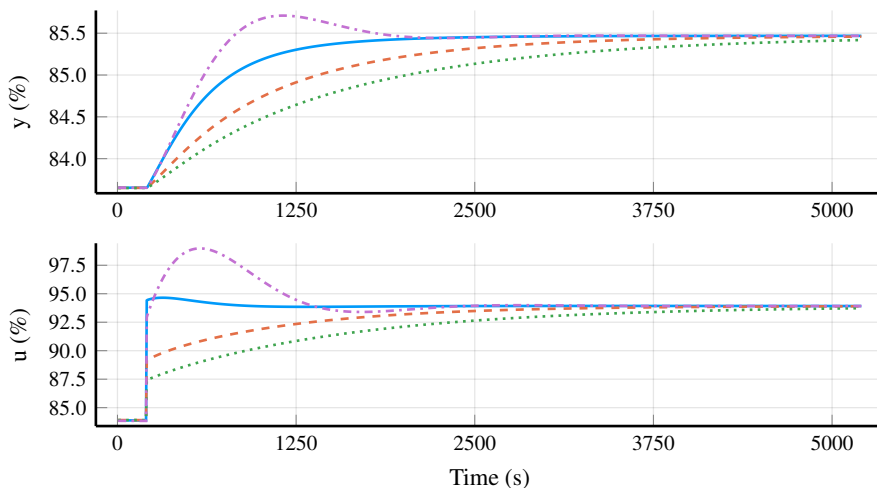


Figure 6.1 SP change on temperature zone 2 in upper combustion area for four different tuned PI-controllers. Upper figure shows the temperature and the bottom figure shows the control signal. The blue solid lines are $\lambda = 1T$, the orange dashed lines are $\lambda = 2T$, the green dotted lines are $\lambda = 3T$ and the purple dashdotted lines are the parameters currently used at Höganäs. Note the large overshoot for the currently used parameters at Höganäs. Both the currently used parameters and the lambda tuned controller with $\lambda = T$ change direction in their control signal.

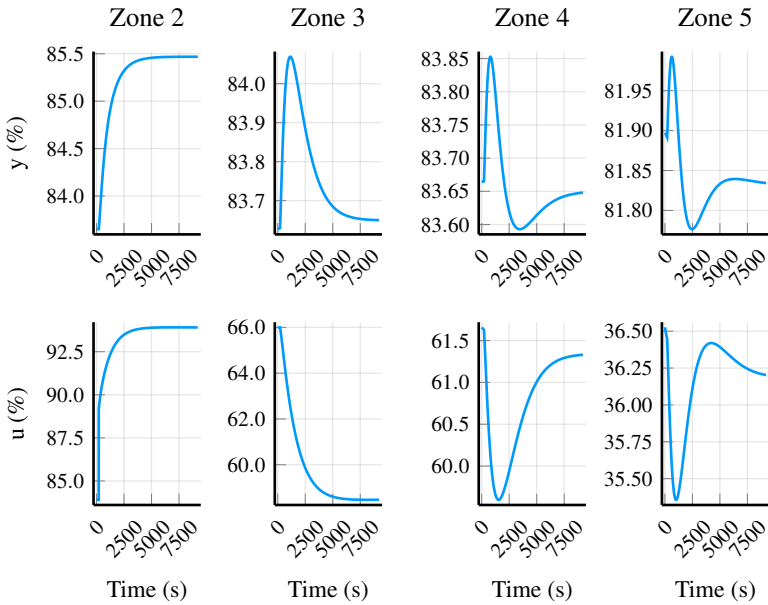


Figure 6.2 SP change on temperature zone 2 in upper combustion area with a lambda tuned controller with $\lambda = 2T$. Zone 2, 3, 4 and 5 are shown and their control signal. The last three zones are not of interest as in the process, their temperatures are far above the SP, thus excluded.

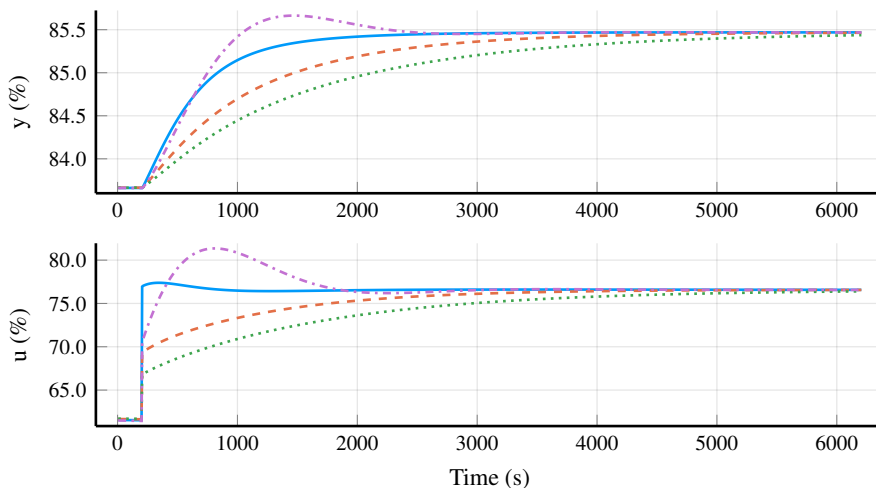


Figure 6.3 SP change on temperature zone 4 in upper combustion area for four different tuned PI-controllers. Upper figure shows the temperature and the bottom figure shows the control signal. The blue solid lines are $\lambda = 1T$, the orange dashed lines are $\lambda = 2T$, the green dotted lines are $\lambda = 3T$ and the purple dashdotted lines are the parameters currently used at Höganäs. Note the overshoot for the currently used parameters at Höganäs. The control signal for both the currently used parameters and the lambda tuned controller with $\lambda = T$ change direction.

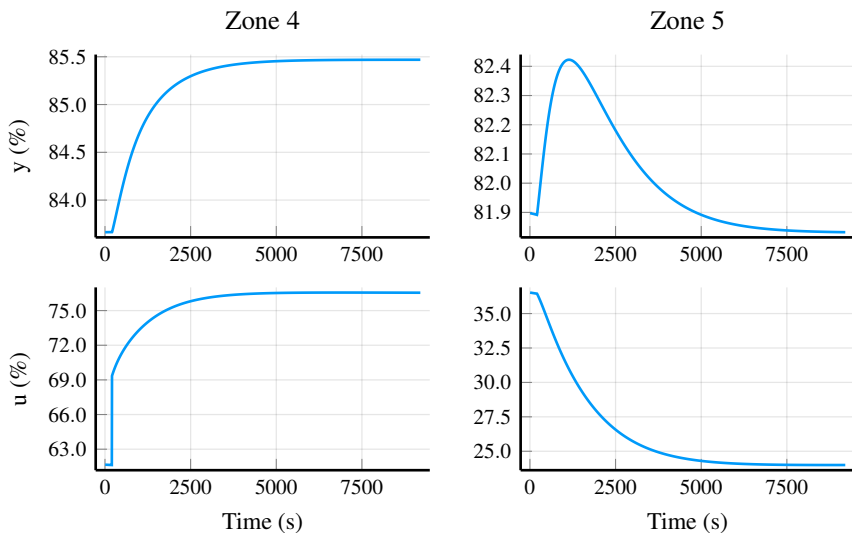


Figure 6.4 SP change on temperature zone 4 in upper combustion area with a lambda tuned controller with $\lambda = 2T$. Zone 4 and 5 are shown and their control signal. The last three zones are not of interest as in the process, their temperatures are far above the SP, thus excluded.

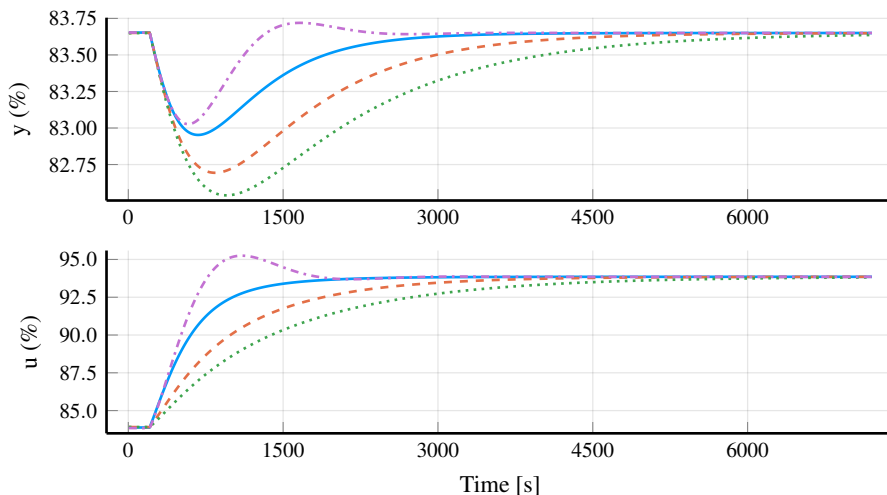


Figure 6.5 The attenuation of a load disturbance on temperature zone 2 in upper combustion area. The blue solid lines are $\lambda = 1T$, the orange dashed lines are $\lambda = 2T$, the green dotted lines are $\lambda = 3T$ and the purple dashdotted lines are the parameters currently used at Höganäs. The corresponding IAE values can be found in Table 6.3.

7

Discussion and Conclusion

The final chapter which covers the comparison between the tested controllers, the most promising tuning principle to apply for the belt furnaces at Höganäs, the accuracy of the model and lastly future work.

7.1 Comparison

As seen in Fig. 5.4, the process has no or barely no dead time. The dead time seen in the first step response could have been caused by the oscillations present, as there is no dead time in the second response.

Therefore the dead time was presumed to be zero (even if $L \neq 0$, $L \ll T$), the tuning principles AMIGO and SIMC were not suitable for the process. Their tuning parameters rely on the dead time for suitable control parameters. In Sec 2.4, a SP change on a FOTD with an AMIGO tuned controller and its output is shown in Fig. 2.5. It introduced an overshoot, which is not sought after in the process as it is unnecessary cost and wear on the equipment. The same behavior can be seen in Sec 2.6 for the SP change on a FOTD with a SIMC tuned controller, see Fig. 2.7. Therefore, the AMIGO and SIMC tuning principles were excluded from the simulations.

The currently used parameters at Höganäs have an integral gain which is too short for the process, see Table 6.1. In Fig. 5.6, the recovery from a belt stop is shown. The oscillations in both the measured value and the control output are not desired and caused by the short time constant. It takes approximately 45 min for the system to stabilize again. The oscillations also have an effect on the succeeding zones.

It is desirable that the controller does not introduce an overshoot during a SP change. The lambda tuning principle with a correct choice of lambda, will not introduce any oscillations in the process since the direction of the control output will not have to change during a SP change. One drawback though is that with a lambda tuned controller the process may be slowed down (if $\lambda > T$). Lambda tuned param-

eters may also have the drawback of poor attenuation of load disturbances, as the controller is not optimized for handling them.

In Fig. 6.1, the four tested controllers are shown. Both the original parameters and an aggressively tuned lambda have an overshoot in the CO. The last two controllers, with more stable and robust choices of lambda have nice and smooth responses. The same behavior is seen in Fig. 6.3.

In Fig. 6.2, one can see how the succeeding zones are affected by the SP change in temperature zone 2 in the upper combustion area with a lambda tuned controller with $\lambda = 2T$. The response is stable and the temperatures does not deviate much from their SP.

The currently used controller at Höganäs has a lower value of IAE than the lambda tuned controller, but has an overshoot.

7.2 Most promising tuning principle

The most promising tuning principle is the lambda tuning principle with a $\lambda = 2T$ since it is stable and does not heavily rely on the dead time for the control parameters. It does not introduce any overshoot for attenuation of load disturbances and SP changes and it is faster than the robust lambda tuned controller with $\lambda = 3T$. The drawback though is the handling of load disturbances. $\lambda = 1T$ could also be an effective choice, but as simplifications were done during the modeling, the aggressive controller could have larger overshoots for SP changes and load disturbances on the process. As the belt stop can be seen as a SP change, rather than a load disturbance, it would be a wiser choice compared to the currently used parameters as it would put less stress and wear on the equipment and make the response smoother. The manual for tuning the controllers at Höganäs can be seen in Appendix D.

7.3 Accuracy of model

The accuracy of the model can greatly be increased by extending the radiation model to cover more of the furnace, i.e. radiation affects adjacent zones. Another part that can increase the accuracy of the whole model is the gas model. By using e.g. Navier-Stokes equation to describe the gas mathematically, it is believed that the model would be more accurate.

7.4 Future work

The performance of the process can be improved with better choices of control parameters for the PID-controllers. As it was not possible to perform a step response analysis of each zone in the belt furnace for the thesis due to time, it should be done. From the step responses, it is possible to try the most promising tuning principle

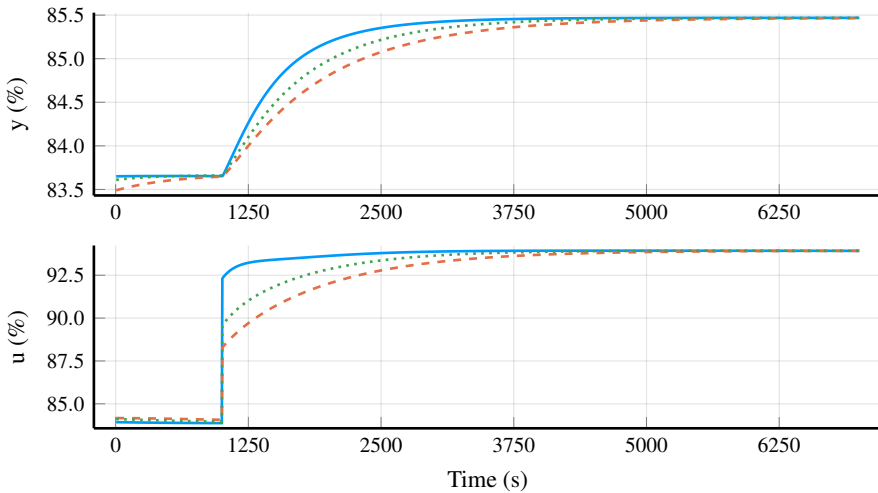


Figure 7.1 SP change on temperature zone 2 in upper combustion area with weighted SP, $b = 0.8$. The temperature is presented in the upper figure and the control signal in the lower figure. All three controllers are lambda-tuned. The blue solid line is $\lambda = T$, the orange dashed line is $\lambda = 2T$ and the green dotted line is $\lambda = 1.5T$.

presented on the belt furnace and see how much it improves the performance. As $\lambda = 2T$ was chosen due to stability, the more aggressive choice of lambda also seemed promising and it is possible to choose a value in between. As the process characteristics only need to be derived once, it is easy to try different choices of lambda to adjust the proportional gain of the controllers. Another option would be to use a setpoint weight to make the control signal smoother for SP changes, see Fig. 7.1. It does not improve the attenuation of load disturbances.

The model was first implemented in MATLAB and Simulink, but later remade in Julia, which opens up for improvements easier. The furnace could be made more generalized with more modules, so that it would be easy to apply the model on any of the belt furnaces at Höganäs to experiment.

More future work would be as mentioned in the previous section, to model the radiation and gas with more accurate models.

Gaussian noise could also be added to the process to see how well the controller handles small variations.

An interesting aspect would be to use the model for optimization of a criteria such as the thickness of the powder, the speed of the belt or the output of the burners to see if it would be more effective to increase the thickness of the powder and decrease the speed of the belt or v.v..

A

View factor

The appendix covers the geometrical figures and the corresponding view factor equation that was used for the thermal radiation in the muffle and combustion areas [*Radiative view factors*].

Two equal parallel plates

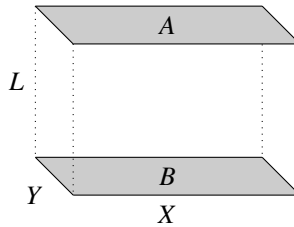


Figure A.1 Two equal parallel plates

$$\begin{aligned}x &= X/L & y &= Y/L \\x_1 &= \sqrt{x^2 + 1} & y_1 &= \sqrt{y^2 + 1}\end{aligned}$$

$$F_{A \rightarrow B} = \frac{1}{xy\pi} \left(\ln \frac{x_1^2 y_1^2}{x_1^2 + y_1^2 - 1} + 2x(y_1 \arctan \frac{x}{y_1} - \arctan x) + 2y(x_1 \arctan \frac{y}{x_1} - \arctan y) \right) \quad (\text{A.1})$$

Two unequal parallel plates

For a rectangular plate to an unequal rectangular plate

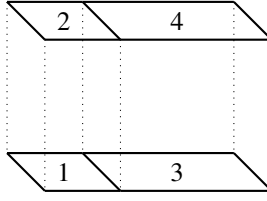


Figure A.2 Two unequal parallel plates

In order to calculate the view factor to an adjacent plate, one can make good use of the reciprocity rule. For Fig. A.2,

$$\begin{aligned}
 F_{(1,3)-(2,4)} &= F_{(1,3)-2} + F_{(1,3)-4} \\
 &= \frac{A_2}{A_1 + A_3} F_{2-(1,3)} + \frac{A_4}{A_1 + A_3} F_{4-(1,3)} \\
 &= \frac{1}{A_1 + A_3} (A_2(F_{2-1} + F_{2-3}) + A_4(F_{4-1} + F_{4-3}))
 \end{aligned}$$

since $A_4 F_{4-1} = A_1 F_{1-4}$ and $F_{2-3} = F_{1-4}$

$$F_{2-3} = \frac{(A_1 + A_3)F_{(1,3)-(2,4)} - A_2 F_{2-1} - A_4 F_{4-3}}{2A_1} \quad (\text{A.2})$$

By extending Fig. A.2 with two more plates,

$$\begin{aligned}
 F_{(1,3,5)-(2,4,6)} &= F_{(1,3,5)-2} + F_{(1,3,5)-4} + F_{(1,3,5)-6} \\
 &= \frac{1}{A_1 + A_3 + A_5} (A_2(F_{2-1} + F_{2-3} + F_{2-5}) \\
 &\quad + A_4(F_{4-1} + F_{4-3} + F_{4-5}) + A_6(F_{6-1} + F_{6-3} + F_{6-5}))
 \end{aligned}$$

since $A_1 F_{1-6} = A_6 F_{6-1}$, $F_{2-5} = F_{1-6}$ and $A_1 = A_2, A_3 = A_4, A_5 = A_6$

$$\begin{aligned}
 F_{1-6} &= \frac{1}{2A_1} ((A_1 + A_3 + A_5)F_{(1,3,5)-(2,4,6)} - A_2(F_{2-1} + F_{2-3}) \\
 &\quad - A_4(F_{4-1} + F_{4-3} + F_{4-5}) - A_6(F_{6-3} + F_{6-5}))
 \end{aligned} \quad (\text{A.3})$$

Two unequal perpendicular plates

$$h = H/L$$

$$w = W/L$$

$$a = \frac{(1 + h^2)(1 + w^2)}{1 + h^2 + w^2}$$

$$b = \frac{w^2(1 + h^2 + w^2)}{(1 + w^2)(h^2 + w^2)}$$

$$c = \frac{h^2(1 + h^2 + w^2)}{(1 + h^2)(h^2 + w^2)}$$

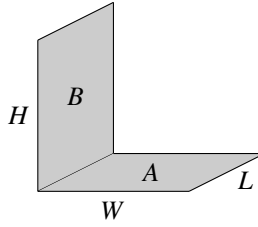


Figure A.3 Two unequal perpendicular plates

$$F_{A \rightarrow B} = \frac{1}{\pi w} \left(h \arctan \frac{1}{h} + w \arctan \frac{1}{w} - \sqrt{h^2 + w^2} \arctan \frac{1}{\sqrt{h^2 + w^2}} + \frac{1}{4} \ln(ab^{w^2}c^{h^2}) \right) \quad (\text{A.4})$$

Sphere to plane

$$r < d \quad D_1 = d/L_1 \quad D_2 = d/L_2$$

$$F_{1 \rightarrow 2} = \frac{1}{4\pi} \tan^{-1} \sqrt{\frac{1}{D_1^2 + D_2^2 + D_1^2 D_2^2}} \quad (\text{A.5})$$

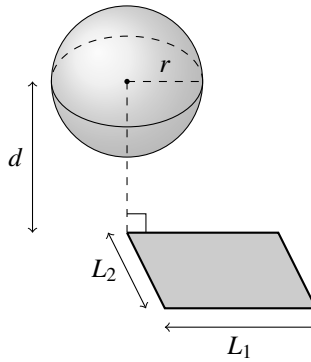


Figure A.4 Sphere to plane

B

Gas composition

The mix of natural gas that Höganäs uses can be seen in Table B.1.

The heating value, H_i , for the mix is $39.75 \text{ MJ}/(\text{Nm}^3)$ ($\approx 11.0 \text{ kWh}/(\text{Nm}^3)$). The amount of fuel needed to reach the full output of a single burner is $10.55 \text{ Nm}^3/\text{h}$.

In order for the natural gas to ignite, oxygen is necessary for the stoichiometric combustion. Theoretically, one would need a certain amount, but practically, one needs to add extra oxygen for full combustion of all the fuel. The excess ratio of added oxygen used is a ratio of $\lambda = 1.2$.

Stoichiometric combustion will need 10.55 Nm^3 air for each Nm^3 of natural gas. By increasing the amount of air by λ it increases the amount of necessary air to 12.67 Nm^3 .

The volume of the fumes generated is thus a total of approximately 13.67 Nm^3 per 1 Nm^3 fuel used.

The specific heat capacity for the fumes is then $1.49 \text{ kJ}/(\text{Nm}^3 \text{ K})$ at $1000 \text{ }^\circ\text{C}$ and $1.32 \text{ kJ}/(\text{Nm}^3 \text{ K})$ at $0.0 \text{ }^\circ\text{C}$

The total amount of fumes generated from a single burner at maximum output is $143.6 \text{ Nm}^3/\text{h}$.

Table B.1 Gas components in the natural gases

Compound	Chemical formula	(%)
Methane	CH_4	89.30
Ethane	C_2H_6	5.80
Propane	C_3H_8	2.40
Butane	C_4H_{10}	1.00
Pentane	C_5H_{12}	0.25
Hexane	C_6H_{14}	0.06
Nitrogen	N_2	0.30
Carbon dioxide	CO_2	0.89
Total		100

Table B.2 Fumes generated at full combustion in "wet" air

Compound	Chemical formula	(%)
Nitrogen	N ₂	72.43
Water	H ₂ O	15.09
Carbon dioxide	CO ₂	8.41
Oxygen	O ₂	3.24
Argon	Ar	0.84
Total		100

C

Isolation materials

Table C.1 Isolation materials in the roof

Material	length [m]
HR140	0.231
Skamolex	0.259

Table C.2 Isolation materials in the floor

Material	length [m]
HR140	0.188
Poros	0.303

Table C.3 Isolation materials in the upper wall

Material	length [m]
HR140	0.230
Skamolex	0.259

Table C.4 Isolation materials in the lower wall

Material	length [m]
HR140	0.235
Poros	0.231
Skamolex	0.160

Table C.5 Physical properties used

Material	ρ [kg/m ³]	C_p [J/(kg K)]	λ [W K/m]
HR140	870	840	0.39
Poros	650	400	0.18
Skamolex	245	840	0.13

D

Manual for tuning the PID controllers (ENG & SWE)

Tuning manual

For tuning the PID-controller at zone X.

Gather data

1. Verify that the furnace has been in normal operation and has been stable for the past 4 h. It is stable if there has not been any periodic disturbances or major temperature changes. If not, wait until the system has been stable for 4 hours.
2. Put the controller in zone X and its adjacent and opposite zones in both upper and lower combustion areas into manual mode.
 - a) Add 5 % to the control output on all zones in manual mode in order to assure that the temperature won't drop below the setpoint and damage the product.
3. Wait 30 min and observe if the temperature in the zones set to manual are stable. If not, wait until they have been stable for 30 min. Note: The temperature should be a couple °C above the setpoint.
4. Increase the control output in zone X with 30 %.
5. Wait for the system to stabilize.
 - a) Observe if succeeding zone also have stabilized.
 - b) Observe if zone X in the opposite area also have stabilized.
6. Decrease the control output in zone X by 30 %.
7. Restore all controllers to auto mode.
8. Export the data for zone X.

Calculation of control parameters Plot the temperature and the control output for zone X for the amount of time that the data gathering took place. To find ΔPV , take the difference of the temperature before the increase of the control output and once it has stabilize after the increase in step 5. Note, if there is noise present, take the mean of the values.

$$\Delta PV = \Delta PV_{\text{after}} - \Delta PV_{\text{before}}$$

ΔCO is the difference between the control output before and after the change made in step 4.

$$\Delta CO = \Delta CO_{\text{after}} - \Delta CO_{\text{before}}$$

It should be 30 %, unless another amount was added to the control output. "range" is the range of temperature measurement for the controller. Calculate the process gain K_p with the following formula

$$K_p = \frac{\Delta PV \cdot 100}{\Delta CO \cdot \text{range}}$$

ΔPV is multiplied by a factor 100 and divided by the "range" in order to present it in percentage.

Find the time when the temperature has increased by $0.63\Delta PV$ after the increase in the control output and take the difference from when the zone first reacts to the increase in the control output. The difference in time is the time constant T .

If the system does not react immediately to the increase in the control output, the difference between the changed output time and the time the system reacts is the dead time L , otherwise $L = 0$.

λ is the design parameter. For a stable response to a setpoint change, let $\lambda = 2T$. By decreasing λ , the response to setpoint changes is faster, but there might be overshoots in the control signal. With the K_p , T , L and λ , use the following formula to calculate the control parameters

$$K = \frac{T}{K_p(L + \lambda)}$$

$$T_i = T$$

Finally, do not forget to update the control parameters in the system.

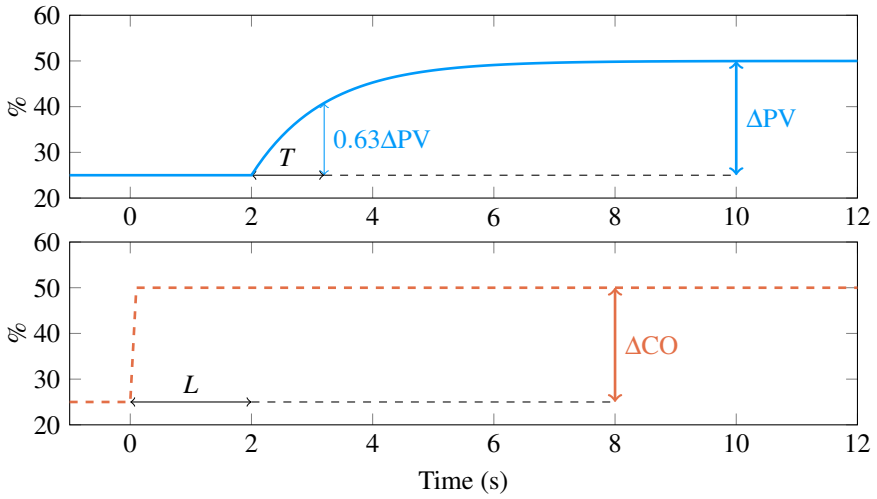


Figure D.1 Graphical representation of ΔPV , ΔCO , T and L . One can see that the process characteristics $L = 2\text{ s}$, $\Delta CO = 25\%$, $\Delta PV = 25\%$ and that at $0.63\Delta PV$ $T = 3.2 - 1 = 1.2\text{ s}$.

Inställningsmanual

För ställa in PID-regulatorn för zon X.

Insamling av data

1. Kontrollera att bandugnen har varit i normal drift och stabil de senaste 4 h. Den är stabil om det inte har varit några periodiska störningar eller större temperaturförändringar. Om inte, vänta tills att systemet har varit stabilt i 4 h.
2. Sätt regulatorn för zon X och dess omgivande zoner i både den övre och nedre förbränningsområdet i manuellt läge.
 - a) Läg till 5 % på styrsignalen för alla regulatorer som är i manuellt läge för att försäkra att temperaturen inte sjunker under börvärdet och skadar produkten.
3. Vänta 30 min och observera ifall temperaturen i zonerna som är satta i manuellt är stabila. Om inte, vänta tills de har varit stabila i 30 min. Notera: Temperaturen borde vara några °C över börvärdet.
4. Öka styrsignalen för zon X med 30 %.
5. Vänta tills att systemet har stabiliserat.
 - a) Observera om efterföljande zoner har stabiliserats.
 - b) Observera ifall zon X på motstående sida har stabiliserats.
6. Minska styrsignalen för zon X med 30 %.
7. Återställ alla regulatorer till auto.
8. Exportera datan för zon X.

Beräkning av regulator parametrar Rita upp temperaturen och styrsignalen för zon X för den tid som det tog för att samla in datan. För att hitta ΔPV , ta differensen av temperaturen innan ökningen av styrsignalen och efter att den har stabiliserats i steg 5. Notera, om signalen är brusig, ta ett medelvärde av värdena.

$$\Delta PV = \Delta PV_{\text{after}} - \Delta PV_{\text{before}}$$

ΔCO är differensen mellan styrsignalen innan och efter ökningen gjord i steg 4.

$$\Delta CO = \Delta CO_{\text{after}} - \Delta CO_{\text{before}}$$

Den borde vara 30 %, såvida inte styrsignalen ökades med ett annat tal. ”range” är intervallet för temperaturmätningar för regulatorn.

Beräkna processförstärkningen K_p med följande formel

$$K_p = \frac{\Delta PV \cdot 100}{\Delta CO \cdot \text{range}}$$

ΔPV multipliceras med en faktor hundra och divideras med "range" för att få värdet i procent.

Hitta tiden då temperaturen has ökat med $0.63\Delta PV$ efter ökningen i styrsignalen och ta differensen med när zonen först reagerar på ökningen av styrsignalen. Skillnaden i tid är tidskonstanten T .

Om systemet inte reagerar omedelbart på en ökning i styrsignalen, differensen mellan tiden för styrsignalens ökning och då systemet först reagerar på ökningen är dödtiden L , annars $L = 0$

λ är designparametern. För en stabil börvärdesändring, sätt $\lambda = 2T$. Genom att minska λ ökar hastigheten på börvärdesändring, med risken för översläng i styrsignalen.

Med K_p , T , L och λ , använd följande formel för att beräkna regulator parametrarna

$$K = \frac{T}{K_p(L + \lambda)}$$

$$T_i = T$$

Slutligen, glöm inte att uppdatera regulatorn i systemet med de nya parametrarna.

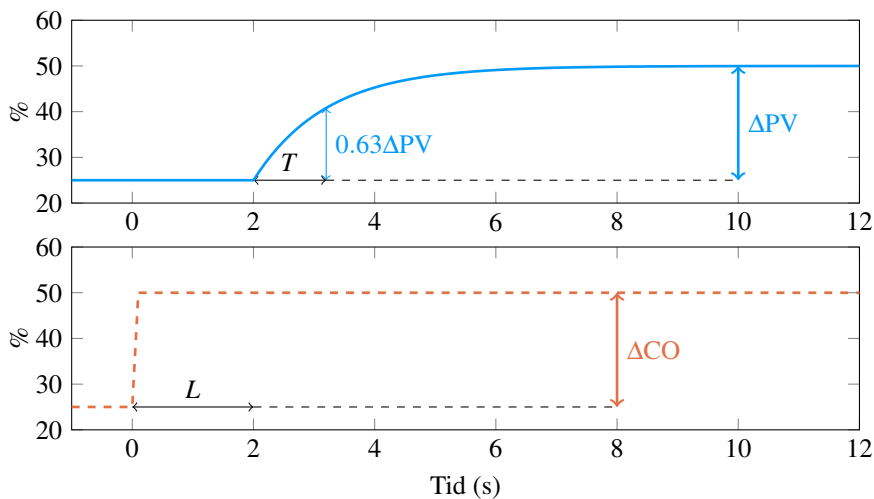


Figure D.2 Grafisk representation av ΔPV , ΔCO , T och L . Man ser att process egenskaperna är $L = 2$ s, $\Delta CO = 25\%$, $\Delta PV = 25\%$ and that at $0.63\Delta PV$ $T = 3.2 - 2 = 1.2$ s.

Bibliography

- Åström, K. J. and T. Hägglund (2006). *Advanced PID control*. ISA - The Instrumentation, Systems and Automation Society.
- Coke (fuel) (2018). *Coke (fuel) — Wikipedia, the free encyclopedia*. [Online; accessed 29-May-2018]. URL: [https://en.wikipedia.org/wiki/Coke_\(fuel\)](https://en.wikipedia.org/wiki/Coke_(fuel)).
- Conveyor belt furnace (2018). *Conveyor belt furnace — Wikipedia, the free encyclopedia*. [Online; accessed 21-Sep-2018]. URL: https://en.wikipedia.org/wiki/Conveyor_belt_furnace.
- Garner, W. (1948). “Radiant energy from flames”. *Proceedings of the Symposium on Combustion* **1-2**, pp. 19 –23. ISSN: 1062-2888. DOI: [https://doi.org/10.1016/S1062-2888\(65\)80005-3](https://doi.org/10.1016/S1062-2888(65)80005-3). URL: <http://www.sciencedirect.com/science/article/pii/S1062288865800053>.
- Hägglund, T. (2013). *Reglerteknik ak*.
- Håkansson, M. and L. Andersson (2007). *Simulering av energibalanser i bandugn - med Matlab och Comsol Multiphysics*. MA thesis. Lunds tekniska högskola.
- Höganäs - About Us (2018). [ONLINE; accessed 29-May-2018]. URL: <https://www.hoganas.com/en/about-us/>.
- Martinez, I. *Radiative view factors*. URL: <http://webserver.dmt.upm.es/~isidoro/tc3/Radiation%20View%20factors.pdf>.
- Nilsson, L. (2011). *Förbränningslära*. [ONLINE; accessed 29-May-2018]. URL: <http://www3.kau.se/kurstorg/files/f/C10B981C1900b16F3EXxPtD7B20D/Forbranningslara.pdf>.
- Sauer, T. (2012). *Numerical Analysis, Second Edition*. Pearson Education, Inc.
- Siegel, R. and J. R. Howell (2002). *Thermal Radiation Heat Transfer, fourth Edition*. [ONLINE; accessed 29-May-2018]. URL: https://books.google.se/books?id=0389yQ0-fecC&pg=PA213&lpg=PA213&dq=poljak+approach&source=bl&ots=7BGc4f7xfN&sig=Rg8ZP2I3Pn-4X7_1MHM6967b56U&hl=sv&sa=X&ved=0ahUKEwjgk9T577HZAhWMy6QKHdRUCXM6AEIKDAA#v=onepage&q=poljak%20approach&f=false.

Bibliography

Sunden, B. (2012). *Introduction to heat transfer*. WIT Press.

Lund University Department of Automatic Control Box 118 SE-221 00 Lund Sweden		<i>Document name</i> MASTER'S THESIS	
		<i>Date of issue</i> September 2018	
		<i>Document Number</i> TFRT-6068	
<i>Author(s)</i> Henrik Fryklund		<i>Supervisor</i> Ola Löfgren, Höganäs Tore Hägglund, Dept. of Automatic Control, Lund University, Sweden Charlotta Johnsson, Dept. of Automatic Control, Lund University, Sweden (examiner)	
<i>Title and subtitle</i> Principles for tuning heat zone controllers in a belt furnace through modeling and simulation			
<i>Abstract</i> <p>In this thesis the heating area of a belt furnace for annealing metal powder has been modeled. The model was extended with PI-controllers for controlling the energy added to the model. It was simulated with differently tuned controllers to test tuning principles for finding suitable control parameters for the process. The most promising tuning principles was then written as a manual with the aim for process engineers at Höganäs AB.</p> <p>The process is running on a daily basis with control parameters that causes unnecessary overshoots and oscillations in the system. With updated and more suitable control parameters, the furnace is believed to be more efficient. Höganäs has several processes of the same type which the manual could be applied to.</p> <p>The process consists of non-linear thermal radiation, conduction and convection. It is very slow and has approximately no dead time, thus excluding many tuning principles that rely on the dead time. The most promising tuning principle to apply is the lambda-tuning principle which is often used in the process industry [Åström and Hägglund, 2006]. Due to the accuracy of the model, the design parameter was chosen to ensure stability and monotonic setpoint changes. The manual can be found in Appendix D.</p>			
<i>Keywords</i>			
<i>Classification system and/or index terms (if any)</i>			
<i>Supplementary bibliographical information</i>			
<i>ISSN and key title</i> 0280-5316			<i>ISBN</i>
<i>Language</i> English	<i>Number of pages</i> 1-66	<i>Recipient's notes</i>	
<i>Security classification</i>			